

POLITECNICO DI TORINO

Automotive Engineering
Master's Degree Program

Master's Degree Thesis

Grinding Process of Alumina Workpiece with Double Disc Vertical Spindle Grinding Machine



Supervisors:

Atzeni Eleonora
Moos Sandro

Candidate:

Wijayakusumah Naufal

Academic Year 2023/2024

Table of Contents

List of Figures	3
List of Tables	5
1. Abstract.....	6
2. Grinding Process	7
2.1. Basic Grinding Operation	7
2.2. Types of Grinding Operation.....	8
2.3. Surface Grinding.....	9
2.4. Grinding Wheels.....	11
2.4.1. Abrasive Types	11
2.4.2. Grain Size	12
2.4.3. Bonding Materials.....	13
2.4.4. Wheel Structure and Wheel Grade.....	14
2.4.5. Specification of Grinding Wheels.....	15
3. Dressing Process	17
3.1. Traverse Dressing with Stationary Diamond Tools.....	17
3.2. Uniaxial Traverse Dressing with Rotary Diamond Tools.....	19
3.3. Cross-axis Traverse Dressing.....	21
3.4. Form-roll/Plunge Dressing	21
4. Coolant.....	23
4.1. Coolant Properties	23
4.2. Types of Grinding Fluids.....	23
4.3. Coolant Supply System	24
5. Case Study	25
5.1. Grinding Machine Specifications	25
5.2. Workpiece Specification	27
5.3. Grinding Wheel Specification.....	28
5.4. Grinding Requirements.....	29
5.5. Dressing Tool Specification	30
6. Mechanics of Self Rotating Double-Disc Grinding Process	31
7. Design of Experiment	36

7.1.	Flowchart of The Experiment.....	36
7.2.	Main Variables of Double-Disc Grinding Machine.....	37
7.2.1.	Grinding Wheel Openings.....	37
7.2.2.	Grinding Wheel Speed.....	41
7.2.3.	Rotary Table Speed.....	41
7.3.	Variables of Experiment.....	41
7.4.	Measuring Devices.....	42
7.4.1.	Flatness Measurement.....	42
7.4.2.	Roughness Measurement.....	43
7.4.3.	Dial Indicator.....	43
7.5.	Exporting the Data for Analysis.....	44
7.6.	Test Measurement Validation.....	47
7.7.	Experiment Results.....	49
7.7.1.	Comparison between Inner and Outer Ring.....	49
7.7.2.	Results of Parameters Set #1 to #4.....	50
8.	Data Analysis.....	51
8.1.	Statistics of The Results.....	51
8.1.1.	Statistics for Internal Flatness.....	51
8.1.2.	Statistics for External Flatness.....	51
8.2.	One-way ANOVA.....	52
8.2.1.	ANOVA of Internal Flatness.....	52
8.2.2.	ANOVA of External Flatness.....	55
8.3.	Process Capability.....	58
8.3.1.	Process Capability for Flatness.....	59
8.3.5.	Process Capability for Step.....	62
9.	Discussion and Conclusion.....	64
	References.....	66

List of Figures

Figure 1. Six basic elements of surface grinding (1).	8
Figure 2. Types of grinding operations (1).....	9
Figure 3. Schematic of horizontal-spindle surface grinder (2).....	10
Figure 4. Different types of surface grinding. (a) Traverse grinding with horizontal-spindle wheel. (b) Plunge grinding with horizontal-spindle wheel. (c) Vertical spindle with rotary table grinder (2).	10
Figure 5. Two types of worktables for the vertical spindle grinder; left: rotary table, right: reciprocating table (3).....	11
Figure 6. Illustration of the structure of a grinding wheel (4).	14
Figure 7. Standard marking for conventional abrasives (2).....	16
Figure 8. Standard marking for superabrasive (2).	16
Figure 9. Typical shapes of single-point dressing tools (1).	17
Figure 10. Examples of standard grit and cluster tool configurations (1).	18
Figure 11. Examples of block dressers for profile dressing alox wheels (1).	19
Figure 12. Dressing parameters for uniaxial traverse process (1).....	20
Figure 13. Various traverse diamond truers (1).....	20
Figure 14. Cross-axis dressing configuration (5).....	21
Figure 15. Dress configurations for diamond form rolls (1).	22
Figure 16. Monzesi Viotto vertical spindle double disc grinding machine.	25
Figure 17. Top and bottom grinding wheels.....	26
Figure 18. Configuration of Viotto Double Disc Grinding Machine.	26
Figure 19. Technical drawing of rotary table for 36 pieces.	27
Figure 20. Technical drawing of rotary table for 72 pieces.	27
Figure 21. Technical drawing of the specimen.	28
Figure 22. Technical drawing of the grinding wheel.....	29
Figure 23. White corundum dressing tool.	30
Figure 24. Cross-axis traverse dressing configuration (Z: Top grinding wheel, W: Bottom grinding wheel, A: Dressing tool).....	30
Figure 25. Schematic of index-carrier setup for double-disc grinding (7).	31
Figure 26. (a) Geometry and (b) kinematics of double disc grinding process (7).....	32

Figure 27. Illustration of workpiece-moment distribution on the wheel-workpiece contact patch (7).....	33
Figure 28. Material removal rate vs. WCR (7).....	34
Figure 29. Workpiece angular frequency vs. WCR (7).	34
Figure 30. Flowchart of the experiment.	36
Figure 31. Rotary table-grinding wheel geometry diagram.	38
Figure 32. Diagram for total opening of the top grinding wheel.....	39
Figure 33. Setting the inclination of the grinding wheel.	40
Figure 34. Longitudinal and transversal axes of the grinding wheel.....	40
Figure 35. Mitutoyo Roundtest RA-2200 roundness tester.	43
Figure 36. TESA 06930015 TWIN-SURF portable roughness tester.....	43
Figure 37. Dial Indicator.....	44
Figure 38. Measurement report.	45
Figure 39. External flatness report.	46
Figure 40. Internal flatness report.....	46
Figure 41. Third-party measurement result.	47
Figure 42. In-house measurement result.	48
Figure 43. Differences of means of internal flatness.....	53
Figure 44. Interval plot of internal flatness.	54
Figure 45. Boxplot of internal flatness.....	55
Figure 46. Differences of means of external flatness.	56
Figure 47. Interval plot of external flatness.....	57
Figure 48. Boxplot of external flatness.	57
Figure 49. Process capability of average flatness.....	59
Figure 50. Process capability of surface finish.....	60
Figure 51. Process capability of parallelism.....	61
Figure 52. Process capability of thickness dimension.	62
Figure 53. Process capability of step dimension.....	63

List of Tables

Table 1. Knoop Hardness of various materials and abrasives (2).....	12
Table 2. Set of parameters for experiment.	41
Table 3. Difference of workpiece thickness between the inner ring and the outer ring.	49
Table 4. Grinding result from all set of parameters tested.	50
Table 5. Statistics for internal flatness.....	51
Table 6. Statistics for external flatness.	51
Table 7. Measurement results of the chosen set of parameters	58

1. Abstract

The work has been done in Monzese S.p.A., an Italian company based in Nova Milanese, Lombardy region, that specializes on designing and manufacturing grinding machines. The aim of this work is to find the right machine setup and combination of parameters to optimize the grinding result and to achieve the desired requirements from the customer. In this case, the customer has requested to machine a ring-shaped disc made from *Alumina* ceramic (Al_2O_3) using a vertical axis double disc grinding machine with rotary table. The workpiece has relatively small dimension with around 40 mm in diameter and 4 mm in thickness. By using the vertical axis double disc grinding machine with rotary table, it is possible to achieve high production rate of around 50 pieces per minute.

The vertical spindle double disc grinding machine has multiple parameters that can be adjusted to achieve the desired machining result, such as the grinding wheel openings, grinding wheel speed, and rotary table speed. Whereas there are other parameters that has been defined by the company's supplier to ensure the best performance, such as the grinding wheel specification, the lubricant type and flow, and the dressing tool.

The customer requirements of the machined workpiece are to ensure the thickness, flatness, and surface finish of the workpiece is within the tolerances: 3.92 – 3.96 mm for the thickness, $< 5 \mu\text{m}$ for the flatness, and 0.15 – 0.30 μm for the surface finish. The measurement is done in the company's measurement lab as well as in different measurement facility and the customer-owned facility to guarantee the precise measurement results.

2. Grinding Process

Grinding in definition means a process of machining by utilising abrasive grinding wheel(s) which rotate at high speed to remove material from the workpiece. The workpiece should have softer material than the grinding wheel itself in order to be machined. The grinding process and the machine can vary for different applications and bespoke to certain workpiece. Modern grinding machines can integrate automated feeding and slide-way motion to allow for complex shapes to be produced without any manual input. Integration of wheel and dressing tool wear algorithms are possible in modern systems. Self-optimization process can also be introduced by utilising monitoring sensors and intelligent control (1).

The high productivity of modern grinding process is driven by the increasing complexity of abrasive applications. There is an increase in grinding wheel typology with the development of cubic boron nitride (CBN) superabrasive, synthetic and natural based diamond abrasive, and sol gel based ceramic abrasive technology. Advancement in grinding fluid and delivery methods of the fluid play apart in achieving higher removal rates while still maintaining the quality. The advancements in this field include factory-centralized delivery systems, shoe nozzles, high-velocity jets, synthetic oils, neat mineral oils, vegetable ester oils, and new additives. There is also development towards environment-friendly manufacturing by utilising minimum quantity lubrication, instead of the more common flood or jet delivery method (1).

Grinding process is usually used when there are some specific demands from the product requirements. The first one being the requirement to produce high quality parts with high accuracy and close tolerance, such as turbine vanes, rolling bearings, silicon wafers, and contact lenses. The other requirement is when high removal rate is needed, such as the production of flutes of hardened twist drills (1). The grinding process is also preferred for machining hard materials such as refractory metals and ceramics.

2.1. Basic Grinding Operation

There are six basic elements involved during the grinding operation: the grinding machine, grinding wheel, workpiece, grinding fluid, atmosphere, and grinding swarf. A dressing wheel is also present to prepare the grinding wheel. While the grinding wheel machines the workpiece, this operation also wears out the grinding wheel itself. Figure 1 shows the surface grinding operation.

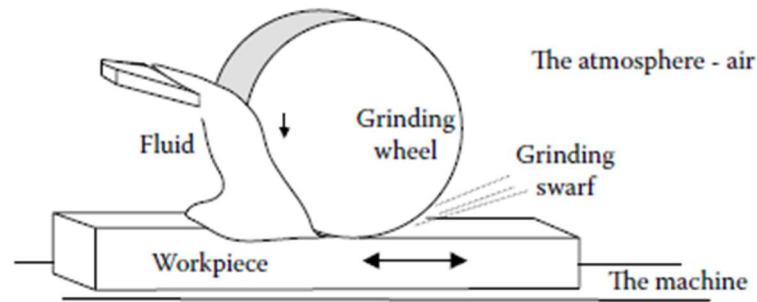


Figure 1. Six basic elements of surface grinding (1).

Grinding swarf is the product of removed workpiece materials combined with grinding fluid residue and worn particles of the grinding wheel. The swarf must be removed by the means of grinding fluid. Grinding fluid acts as lubricant during the grinding process to reduce friction and wear of the grinding wheel. The fluid also acts as coolant to increase the cutting accuracy by limiting the thermal expansion of the workpiece as well as the machine, and to prevent thermal damage to the workpiece. The atmosphere can affect the grinding process of metals by reducing friction. The interaction between the atmosphere and newly exposed metal surface creates an oxidation phenomenon that helps to lubricate the process. The grinding machine should give a stable and stiff platform for the grinding operation in order to achieve accurate and precise geometry, size, roughness, and flatness (1).

2.2. Types of Grinding Operation

There are many types of grinding machine, depending on the shape of workpiece and production rate. The four most common types of grinding processes are (1): peripheral surface grinding, peripheral cylindrical grinding, face surface grinding, and face cylindrical grinding. The difference between peripheral grinding and face grinding is that during peripheral grinding, the axis of the grinding wheel is parallel to the machined surface, whereas in face grinding, the axis of the grinding wheel is normal to the machined surface. The term surface grinding usually refers to grinding flat or profiled surfaces with a linear feed. Cylindrical grinding refers to grinding a rotating workpiece, which can be performed on the internal or external periphery of the workpiece.

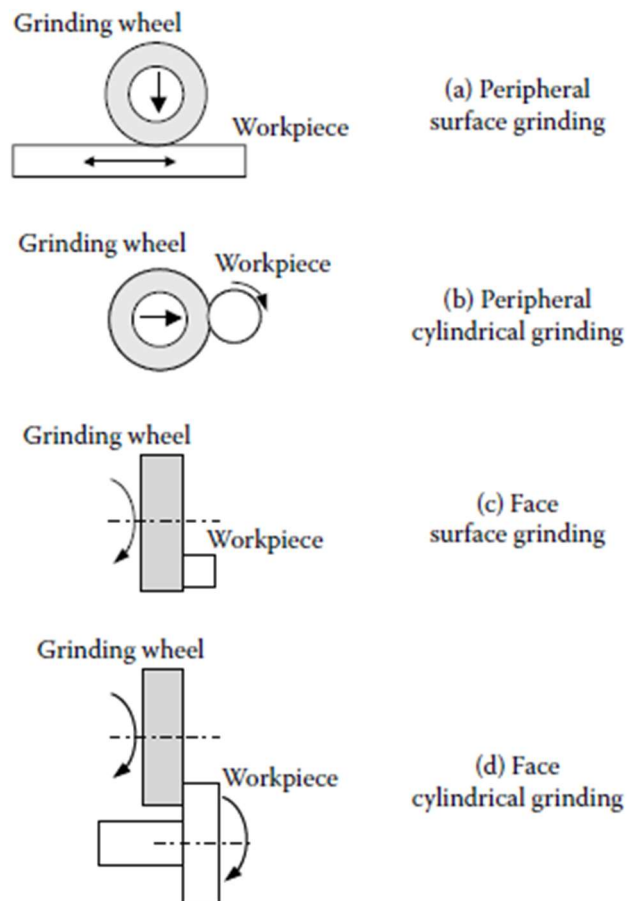


Figure 2. Types of grinding operations (1).

In application, the grinding operation is not limited to these four common types, there are also profiling process such as grinding of spiral flutes, screw threads, spur gears, and helical gears that is similar to cutting operation.

2.3. Surface Grinding

Surface grinding generally involves grinding flat surface, with the grinding wheel mounted on horizontal spindle. *Traverse grinding* process involves reciprocal motion of the table on the longitudinal direction, while the material feed moves in lateral direction (in the direction of the spindle axis) (2). The workpiece is held onto the worktable using magnetic chuck, or vises, vacuum chuck, other fixtures for nonmagnetic materials. Figure 3 shows the schematic illustration of a horizontal-spindle surface grinder.

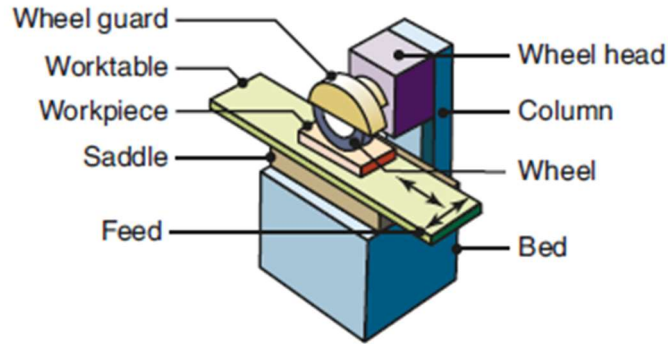


Figure 3. Schematic of horizontal-spindle surface grinder (2).

The grinding wheel movement with respect to the workpiece can be along the surface such as *traverse grinding*, *through-feed grinding*, or *cross-feeding*, or it can be radially into the workpiece such as *plunge grinding* (2). Grinding a groove is one of the examples of *plunge grinding*. Other types of surface grinding are using vertical spindle grinding wheel with either reciprocating table or rotary table. Figure 4 shows the illustration of different types of surface grinding. These configurations allow for multiple pieces to be ground at the same time. Vertical spindle with rotary table grinding machine has high production rate compared to the other types of grinding machines. Figure 5 shows the typology of worktable applicable for vertical spindle grinder.

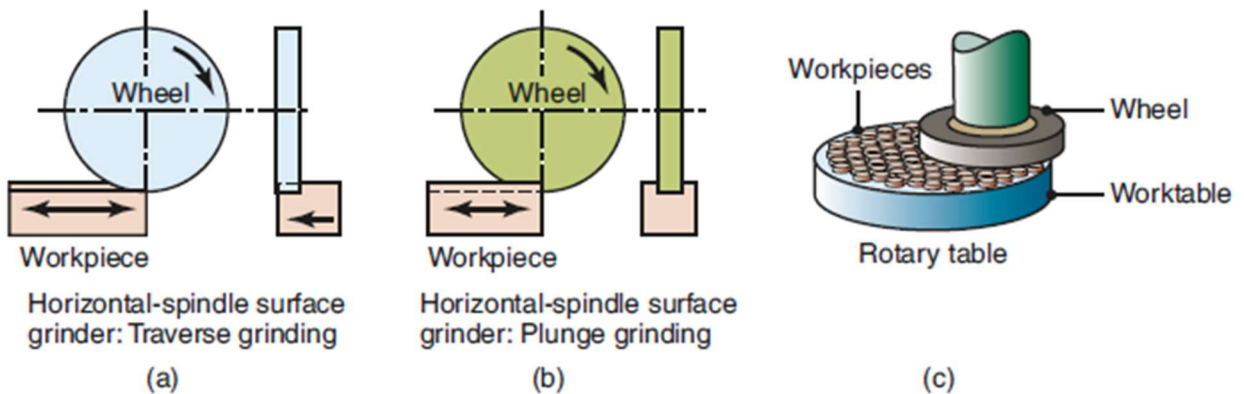


Figure 4. Different types of surface grinding. (a) Traverse grinding with horizontal-spindle wheel. (b) Plunge grinding with horizontal-spindle wheel. (c) Vertical spindle with rotary table grinder (2).

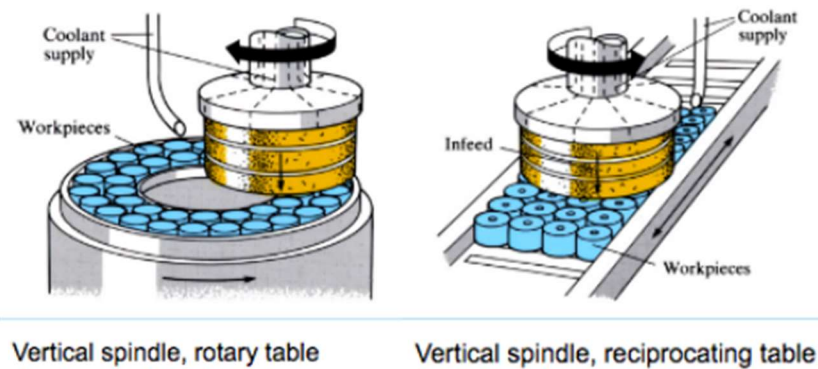


Figure 5. Two types of worktables for the vertical spindle grinder; left: rotary table, right: reciprocating table (3).

2.4. Grinding Wheels

The advancement in the technology of grinding wheel in recent time leads to significant increase in productivity. The application of conventional abrasives and superabrasives with high wheel speed results in increasing of material removal rates by 10 to 100 times compared to low grinding wheel speeds employed in the early twentieth century (1). These high wheel speeds must be taken into account when designing both the grinding wheel and the machine. A much greater wheel strength, new grinding wheel assembly, truing and dressing process, coolant delivery and coolant formulation, and new grinding machine design are necessary to achieve the high wheel speed.

2.4.1. Abrasive Types

The type of abrasives used in grinding wheel can be divided into two main categories: conventional abrasive and superabrasive. One of the distinctive characteristics of abrasive is that it has much higher hardness compared to conventional cutting-tool materials. Table 1 shows some examples of material hardness. Other than the hardness, friability also plays an important role on the characteristic of the abrasive. Friability defines the ability of abrasive grains to break into smaller pieces. This characteristic is essential to give the grinding wheel its self-sharpening property and to maintain its sharpness over time. High friability means the abrasive grains have higher tendency to break under grinding force. the friability of an abrasive grain is affected by its size and shape. Blocky-shaped grains are harder to break or have low friability compared to a plate-like grains. Smaller size grains also have low friability than the larger ones because the probability of grain defects is lower (2).

Table 1. Knoop Hardness of various materials and abrasives (2).

Material	Knoop Hardness
Common glass	350-500
Flint, quartz	800-1100
Hardened steels	700-1300
Aluminium oxide	2000-3000
Silicon carbide	2100-3000
Cubic boron nitride	4000-5000
Diamond	7000-8000

The naturally occurring abrasives in nature contain impurities and have nonuniform properties which lead to inconsistent and unreliable performance. The types of abrasives commonly used in the industry are made synthetically, such as (2):

- Aluminium oxide
- Seeded gel
- Silicon carbide
- Cubic boron nitride
- Diamond

2.4.2. Grain Size

The grain or grit size of the abrasive particle is selected based on the desired material removal rate and the surface finish of the workpiece. Small grit size produces finer surface finish, while large grit size allows for high material removal rate. The hardness of the work material should also be taken into consideration in choosing the right grit size. Soft materials require larger grit size, whereas hard materials require smaller grit size to cut effectively.

Grain size is measured by screening mesh technique. The number of openings of the screen mesh will determine the grain size classification. Small grain size can pass through small mesh openings, and with small mesh openings, there are higher mesh count per linear inch compared to larger openings. Hence smaller grit sizes have larger numbers and vice

versa. The typical range of grain size used in grinding wheels is between 8 to 250. For lapping and superfinishing, finer grain sizes are used (4).

2.4.3. Bonding Materials

Bonding material is used to hold the abrasive grains together in the grinding wheel. the bonding material acts as braces to support the abrasive grains and to provide clearance between the grains. This clearance is also called porosity, which is essential to prevent the interference of chips during the grinding process. The types of bonds that are commonly used are (2):

- Vitrified

Also called ceramic bond, is the most common and widely used bond material. This bond is made of *feldspar* (a crystalline mineral) and clays, which then mixed with abrasives. The bonded abrasive is then moistened and moulded under pressure into grinding wheel shape and baked slowly to a temperature of around 1250°C to fuse the glass together. After the baking process, the wheel is cooled slowly to prevent temperature gradient between the core and the surface of the wheel. this type of grinding wheels is strong, stiff, resistant to oils, acids, and water. The downside is that they are brittle and lack of mechanical and thermal shock. Some vitrified wheels are made with steel-backing plates or cups to improve their strength.

- Resinoid

Resinoid bond is made of thermosetting resins. The grinding wheels with resinoid bonds are also called organic wheels, because of the organic compound used in the bond. To make this abrasive bond, abrasive grains are mixed with liquid or powdered phenolic resins and additives, which then is pressed into grinding wheel shape and cured at temperature of around 175°C to set the resin. Resinoid wheels are more flexible than vitrified wheels because of lower elastic modulus of the resin compared to glass. *Polyimide* is also used as a replacement for the phenolic resin because of its higher strength and higher temperature resistance.

- Reinforced wheels

One or multiple layers of fiberglass mats with various mesh sizes are used in these types of wheels. The fiberglass acts as a lamination structure to prevent the wheels

from disintegrating during its use. Internal rings made of steel bars can also be inserted during the moulding process of the wheel to further improve its strength.

- Rubber

It is the most flexible bonding material used in abrasive wheels. This abrasive bond is made by combining crude rubber, sulphur, and abrasive grains together. The mixture is then rolled into sheets and cut into various diameters. The disks are heated under pressure to vulcanize the rubber. These disks are usually used like circular saws for cutting-off operation.

- Metal

Diamond or cubic boron nitride are usually used as the abrasive grains to be bonded to the periphery of a metal wheel using powder-metallurgy techniques to depths of up to 6 mm. the bonding of metal is done under high temperature and pressure. The core of the grinding wheel can be made of aluminium, bronze, steel, ceramics, or composite materials. The core material will determine its strength, stiffness, and dimensional stability. Another technique is to plate or braze a single abrasives layer onto a metal wheel, which can reduce the cost for small production batches.

2.4.4. Wheel Structure and Wheel Grade

Wheel structure is the relative spacing of the abrasive grains in the wheel. Grinding wheel contain air gaps or pores alongside the abrasive grains and bonding material. This composition can be expressed as (4):

$$P_g + P_b + P_p = 1.0$$

Where P_g = proportion of abrasive grains with respect to the total wheel volume, P_b = proportion of bonding material, and P_p = proportion of pores.

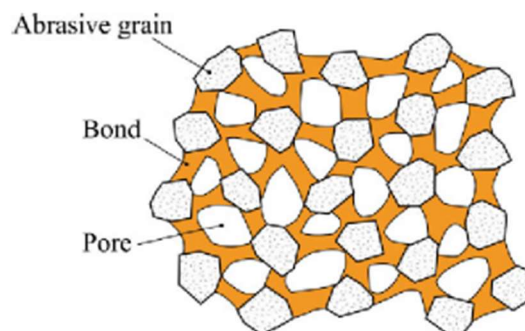


Figure 6. Illustration of the structure of a grinding wheel (4).

Figure 6 represents the structure of a grinding wheel. The scale in which the wheel structure is measured has range between “open” and “dense.” Open wheel structure refers to higher pores proportion per unit volume compared to the abrasive grains proportion, and the opposite for the dense wheel structure. Open wheel structure is generally recommended when grinding materials that requires clearance for the chip. Dense wheel structure is recommended to achieve better dimensional control and fine surface finish (4).

Wheel grade is the scale that measures the grinding wheel’s bond strength to retain the abrasive grains during grinding process. This characteristic is largely affected by the amount of bonding material in the wheel structure. Wheel grade has a scale that ranges between “soft” and “hard.” Soft wheels have the tendency to lose the grains more easily, whereas the hard wheels tend to retain the grains. Soft wheels are used when the work material is hard and small material removal rates is required. Hard wheels are generally used for high material removal rate and for machining relatively soft work materials.

2.4.5. Specification of Grinding Wheels

To differentiate grinding wheels based on their materials and properties, a standardized system consists of letters and numbers is made to indicate the type of abrasive, grain size, grade, structure and bond type of the grinding wheel (2). This system is divided into two categories, for conventional abrasives as shown on Figure 7, and for superabrasives shown on Figure 8.

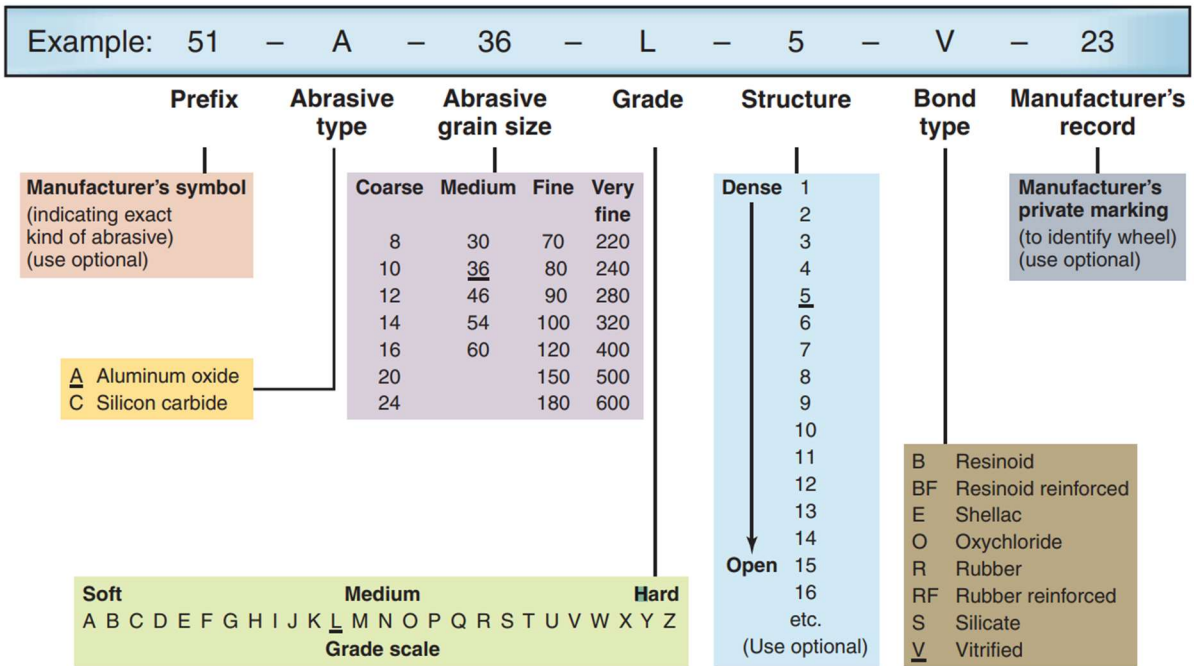


Figure 7. Standard marking for conventional abrasives (2).

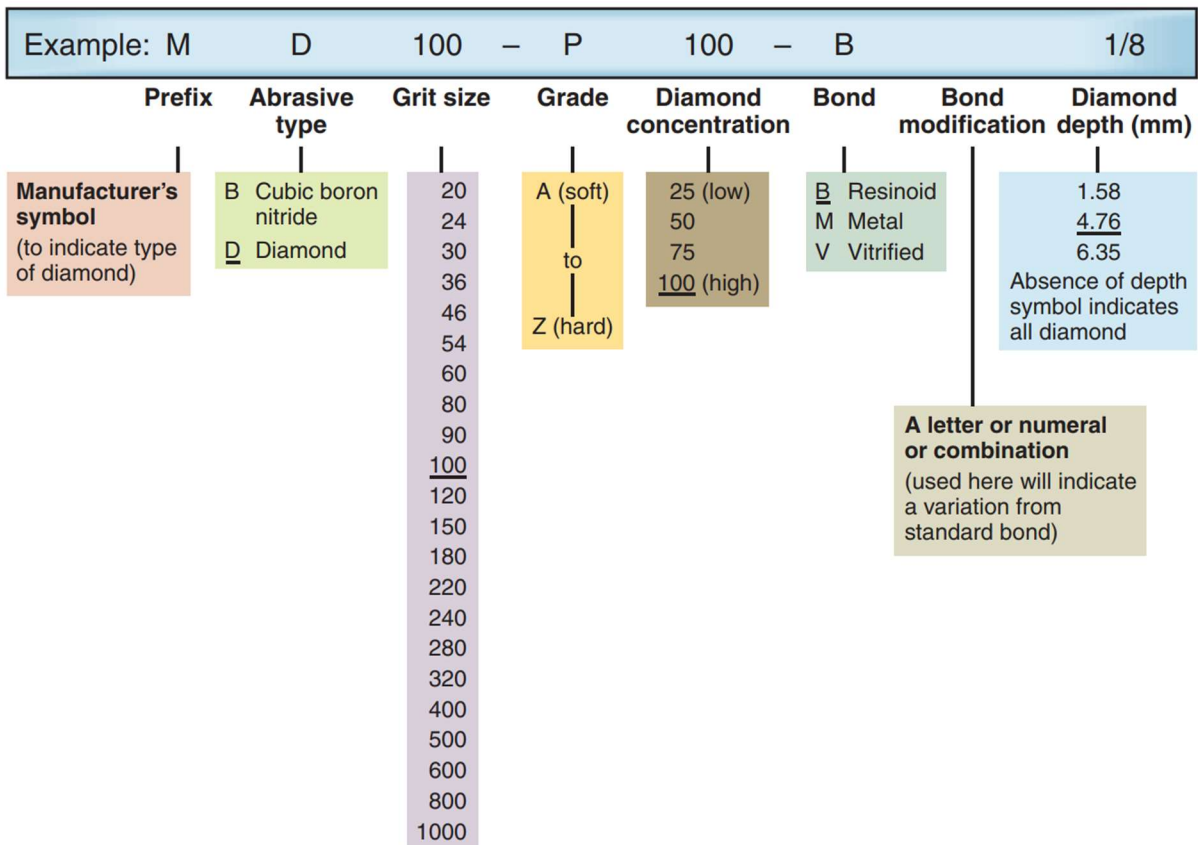


Figure 8. Standard marking for superabrasive (2).

3. Dressing Process

There are many terminologies referring to the process of restoring the surface of a grinding wheel, such as truing, conditioning, and dressing. To understand the difference between them, here is the definition of each term (1):

- Truing: shaping a circular wheel concentric to the axis of wheel rotation, generating a profile on the face of the wheel, cleaning out work material chips that has been embedded during the machining process, and obtaining new, sharp cutting edges on the cutting surface of the wheel.
- Conditioning: preferential bonding material removal from around the abrasive grains.
- Dressing: both truing the wheel and conditioning the cutting surface to acquire an adequate cutting performance of the wheel.

There are two types of dressing process for conventional wheels, dressing with stationary diamond tools and dressing with rotary diamond truers. The later can offer much longer tool life.

3.1. Traverse Dressing with Stationary Diamond Tools

The most basic dressing tool is the single-point diamond. This type of tool usually has an A-shaped profile with rough unlapped diamond on its corner. This corner is well enough defined to be able to repeatedly dress flat wheel forms. This tool is usually the most cost-effective choice even with high initial cost.

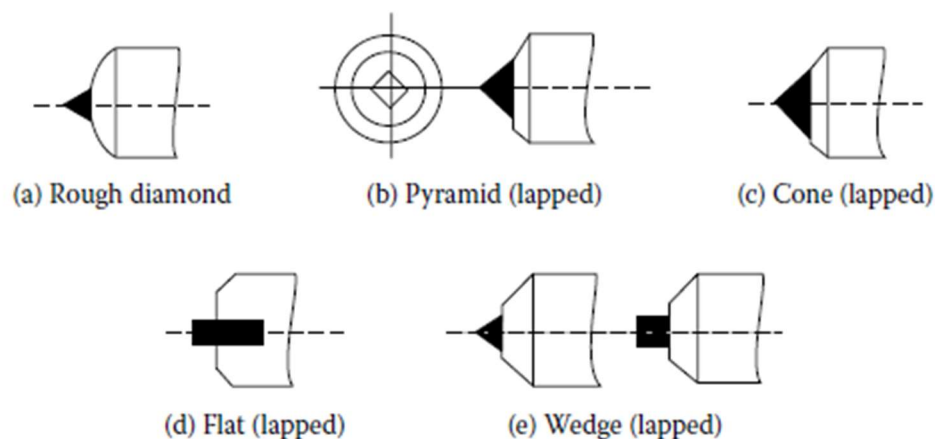


Figure 9. Typical shapes of single-point dressing tools (1).

Single-point tools wear much quicker relative to multi-point dressing tools. The tool loses its sharpness as it wears out, which can affect the grinding process to become inconsistent, and increase of workpiece roughness. There is also possibility of dressing chatter due to vibration of the diamond inside the tool which lead to poor wheel topography and chatter marks.

There are other types of stationary dressing tools also used in the industry. Chisel-shaped tools are used for profiling applications such as profile dressing units for *Diaform* (1). These profiling tools have well-defined radii to generate a particular profile on the wheel.

Grit tools and cluster impregnated tools are used for the roughest dressing of large cylindrical or centreless wheels. Grit tools consist of diamond grain layer held in sintered metal matrix which is highly wear resistant. As the tool wears progressively over time, it will expose new layer of diamond grains. Cluster tools consist of a single layer of five to seven large natural diamonds semi-exposed on a round, flat surface held in sintered metal matrix. These types of tools are cheap, easy to make, and long-lasting, with the downside of less consistent dressing result compared to single-point tools, but generally it is still acceptable.

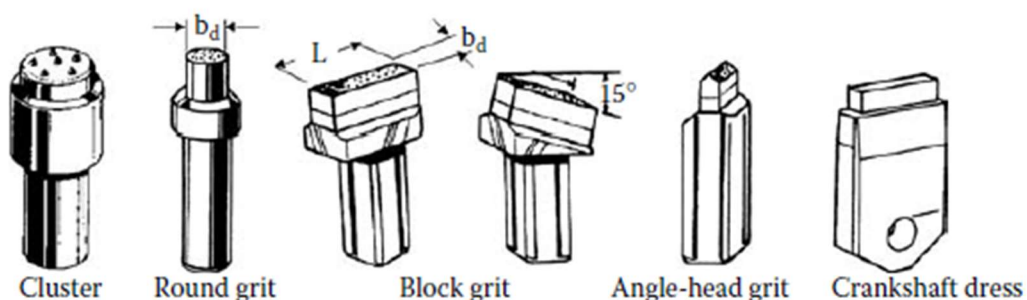


Figure 10. Examples of standard grit and cluster tool configurations (1).

Form blocks are used when simultaneous dressing process of full forms is necessary. A diamond layer is sintered or plated directly on blocks which are moulded to the form required on the wheel. The typical usage of these blocks is for surface grinding in which the block is set on the same height as the finished ground height. The reciprocating stroke length is set in order to dress the wheel before it finishes the grinding process. The blocks can be moulded to follow the full form required or supplied as standard shapes.

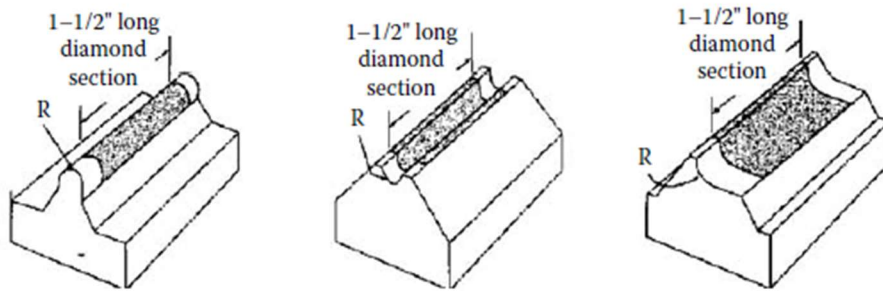


Figure 11. Examples of block dressers for profile dressing alox wheels (1).

3.2. Uniaxial Traverse Dressing with Rotary Diamond Tools

Rotary diamond tool consists of a disc with diamond held on the periphery and driven on a powered spindle. Life of the tool is significantly increased because of more diamond content, which means more cutting edges available. The rotary motion also gives another benefit, which is the relative speed of the dressing tool with the grinding wheel, known as the dressing speed ratio or crush ratio. The crush ratio has significant impact on the dressing process of the wheel. Crush ratio (q_d) is the ratio between the surface speed of the dresser and the wheel (1):

$$q_d = \frac{v_d}{v_s}$$

In a unidirectional crush ratio, the linear speeds of the grinding wheel and the dressing tool on the contact patch are on the same direction, thus the crush ratio has positive sign. For unidirectional dressing, it is recommended to not exceed +0.8 crush ratio to prevent significant dresser wear. For most application, the dresser run in counter directional way, in the range of -0.4 to -0.8.

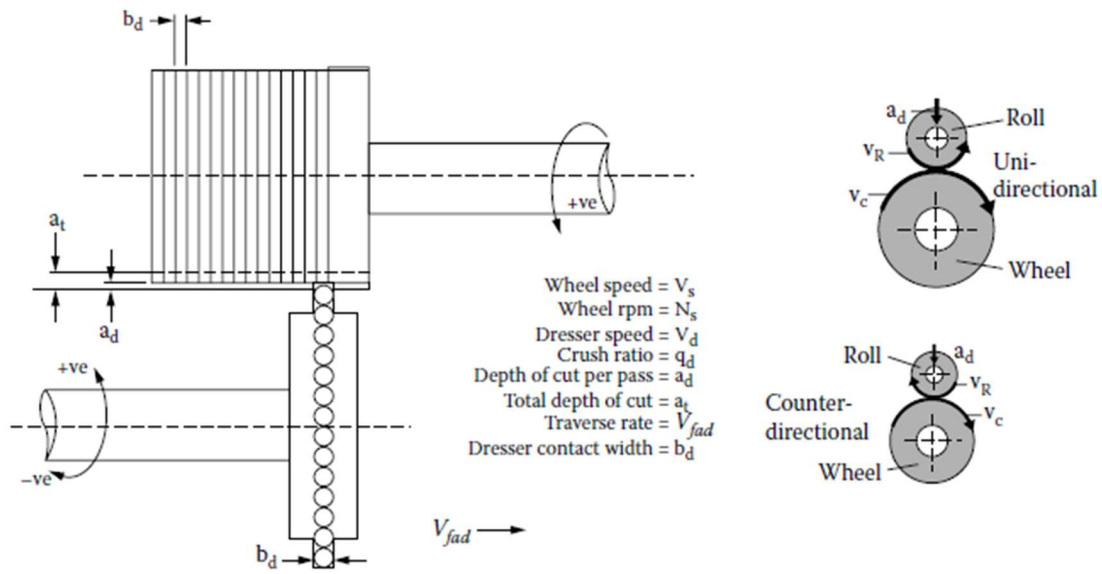


Figure 12. Dressing parameters for uniaxial traverse process (1).

In rotary dressing, there might be an issue of unbalance rotation of the dresser which can lead to chattering and “orange-peel” appearance of the grinding wheel. The chatter phenomenon can be induced by fractional multiples of the dresser-grinding wheel rpm and should be avoided.

There are many types of rotary dressers available. Synthetic diamond discs offer the best longevity with the possibility to be relapped up to 40 times if the wear is properly monitored but have high initial cost. The less expensive alternative is sintered and impregnated rolls. This type of dresser consists of diamond abrasive grains moulded into a layer. The sintered rolls may be relapped two to three times. Another low cost, throw-away alternative is direct-plated diamond with similar profiles to sintered rolls.

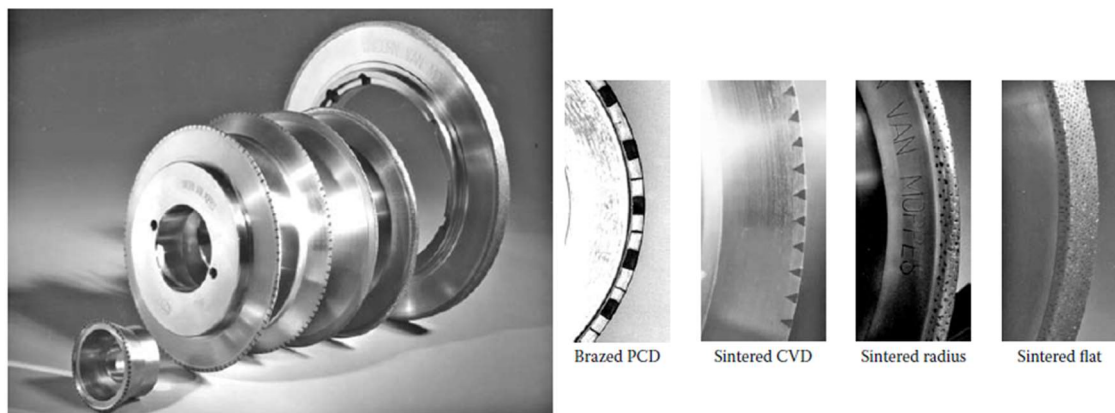


Figure 13. Various traverse diamond truers (1).

3.3. Cross-axis Traverse Dressing

Cross-axis dressing is often considered as a poor dressing process. It has been used in situation where the space inside the machine does not allow for adequate dresser spindle motor for the required torque to operate in uniaxial orientation, or in situation where it is simply impossible to orientate the dresser spindle as such. This configuration allows for axes of the dresser spindle and the grinding wheel to be positioned perpendicular to one another. The dressing action only produces shear force; thus, it is not as effective as uniaxial dressing method (1). The benefit of cross-axis dressing is that it is the most cost-effective method of profile dressing where the contour allows its use. Another benefit is that it gives clearance to dress profiles of over 180°.



Figure 14. Cross-axis dressing configuration (5).

3.4. Form-roll/Plunge Dressing

Traverse dressing of profiles has a drawback, which is cycle time. To achieve rapid dress time, modern high-production grinding machine uses dressing process in which the truer is plunged into the conforming profile. There are two categories of rotary form truers (1):

- RPC (Reverse Plated Construction) rolls, produced by electroforming process,
- Infiltrated rolls, produced by high temperature furnacing.

The dressing process involves plunging the roll into the grinding wheel at fixed infeed rate (mm/min or mm/revolution of the wheel) at fixed crush ratio and fixed dwell time. Figure 15 shows three configurations of the dress infeed. The first configuration is parallel plunge, where the axes of the wheel and roll are aligned. This method is the easiest for designing the roll and checking the form accuracy, but the downside is that it can cause burning and corner

breakdown on the wheel surfaces that are perpendicular to the axis. The next configuration, the angle approach, can minimize the burning effect by optimizing the angle of approach of the roll. The final configuration is a mix of angle approach with traverse method or “wipe.” The wipe movement is done to minimize dressing resistance, improve surface finish, and to prolong the roll life.

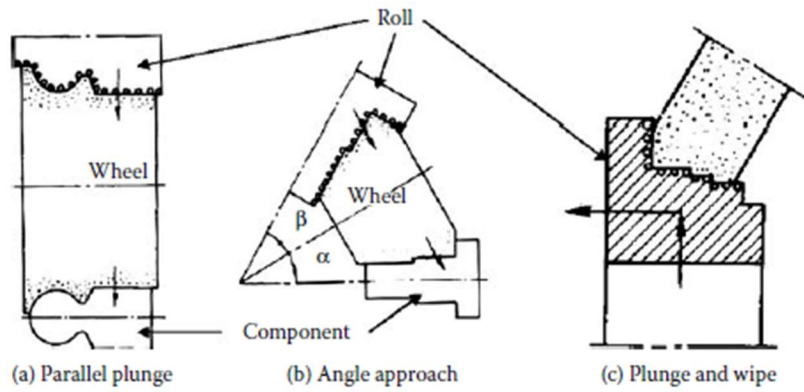


Figure 15. Dress configurations for diamond form rolls (1).

4. Coolant

Coolant is a general term used to define grinding fluids that is utilized during the grinding process to cool and lubricate the abrasion process between. The grinding fluid lubrication property reduces friction between the abrasive grains and workpiece, and between the bond and the workpiece. While the cooling property absorbs and transports the heat generated during grinding (1).

4.1. Coolant Properties

Good grinding fluids should have basic requirements such as good lubrication, good cooling, high flushing performance, and high corrosion protection. The other requirements are environmentally friendly, cheap and efficient to operate, and long lasting. Excellent grinding fluids must also fulfil the additional requirements, such as (1):

- Easy to filter and recycle
- Residual layer is easy to remove
- Excellent solid particle transport for removal of swarf
- Reduces foaming and formation of mist
- Low flammability
- Good compatibility with the materials of the machine

Physical and chemical properties of the grinding fluids can significantly affect their functional and operational behaviour. The ratio of the base material of the grinding fluid also influences the viscosity, heat capacity, evaporation heat, and conductivity of the grinding fluid itself.

4.2. Types of Grinding Fluids

Based on DIN 51 385 Standard, grinding fluids can be classified into three categories:

- Water-immiscible: generally not mixed with water.
- Water-miscible: emulsifiable, emulsifying, or water-soluble concentrates, water is added before use.
- Water composite fluids: ready-to-use coolant, water-miscible lubricant with water included.

For the water-miscible cooling lubricant, there are three categories as well (1):

- Oil-in-water emulsion
- Water-in-oil emulsion
- Cooling lubricant solution

The categorization within the water-miscible cooling lubricants is performed based on the content of active substances or to droplet size in rough, fine, fine colloidal, micellar, and molecular disperse emulsions. The differences within the water-immiscible cooling lubricants are based on the fraction and the type of the active substances contained.

The base material for grinding fluids is natural and synthetic hydrocarbons such as mineral oils, synthetic/vegetable ester, poly-alfa-olefins, or polyglycols. Additives are also added to the fluid to increase its lubricating properties and pressure absorption capacity, such as chemically active Extreme Pressure (EP), substances, or polar agents. Corrosion, foam, and oxidation inhibitors or anti-fog additives are also added to water-immiscible and water composite fluids.

4.3. Coolant Supply System

The coolant supply system must deliver continuous flow of grinding fluid to the wheel-workpiece contact zone during the grinding process. The system should also be able to store and transport the grinding fluid while keeping constant quality, temperature, and adequate quantity to ensure the lubricating, cooling, flushing, and chip transport. Coolant supply system generally comprises of components to distribute the fluid (pumps, pipes, nozzles), return system (channels), maintenance devices (filters, reservoirs, monitoring devices), and equipment for swarf treatment (centrifuges, cleaning nozzles). The design of coolant supply system depends on the required flow and pressure of the fluid leaving the nozzle. Total volume of the fluid to be supplied can be calculated based on the nozzle form, its positioning, and required fluid pressure.

The grinding result is highly influenced by the characteristics and the performance of the coolant nozzle. In general, it is possible to differentiate between the types of nozzle systems into three classifications (1):

- By function (flooding, not flooding)
- By jet pattern (free jet nozzle, point nozzle, swell nozzle, spray nozzle)
- By nozzle geometry (squeezed pipe, needle nozzle, shoe nozzle)

5. Case Study

On this chapter, the grinding machine specification and workpiece requirements are explained. The grinding and dressing wheel choices for this specific grinding operation are also explained.

5.1. Grinding Machine Specifications

The grinding machine used for this machining is vertical spindle double-disc with rotary table. The machine has two grinding wheels, on the top and bottom of the workpiece, which enables it to simultaneously grind both workpiece's top and bottom surfaces. The workpiece is placed on a rotary table that continuously rotates which not only deliver the workpiece, but also regulates the rate of material removed. This type of machine has the capability of continuous operation and high production rate, which the customer requested to achieve at least 50 pieces per minute.



Figure 16. Monzesi Viotto vertical spindle double disc grinding machine.



Figure 17. Top and bottom grinding wheels

Figure 18 illustrates the configuration of the machine and the direction of rotation of the top wheel, bottom wheel, and the rotary table. The top and bottom wheels rotate on the opposite direction and can be controlled independently. The loading and unloading of the workpiece during the test were done manually, but in the final configuration conveyor belt will be utilised for fully automated system.

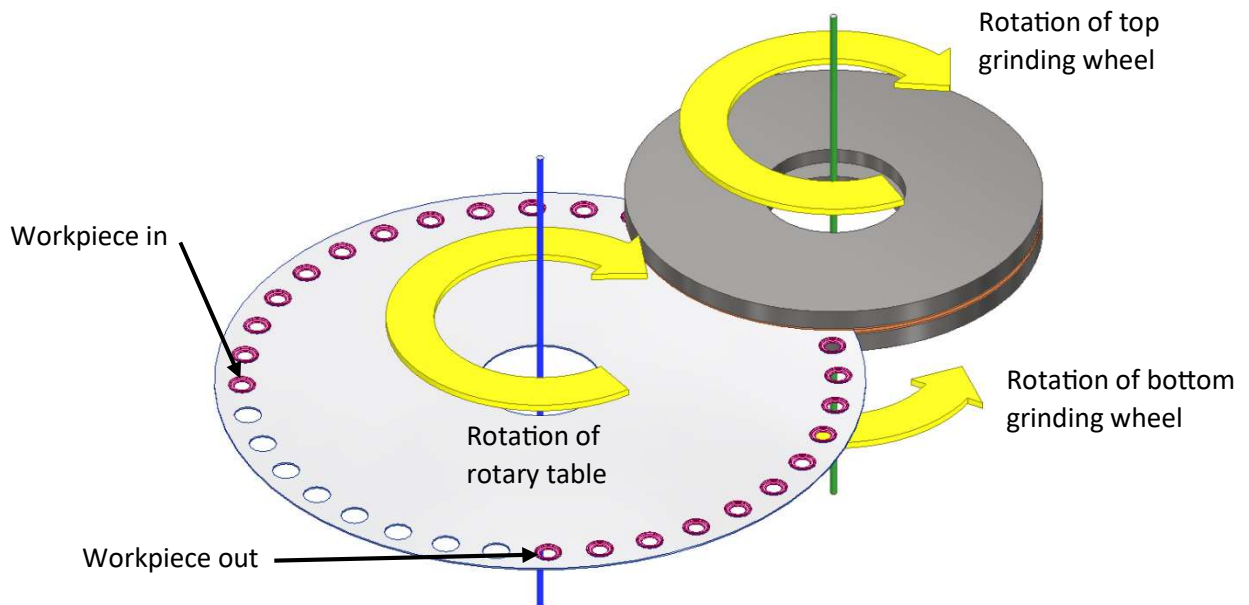


Figure 18. Configuration of Viotto Double Disc Grinding Machine.

The rotary table has been designed to hold 36 pieces at the same time, as shown in Figure 19. To achieve at least 50 pcs/min production rate, it is possible to modify the rotary table

angular speed to increase the machine production output. The rotary table with inner and outer ring capable of holding 72 pieces has also been designed to explore the option of increasing the machine production, as shown in Figure 20.

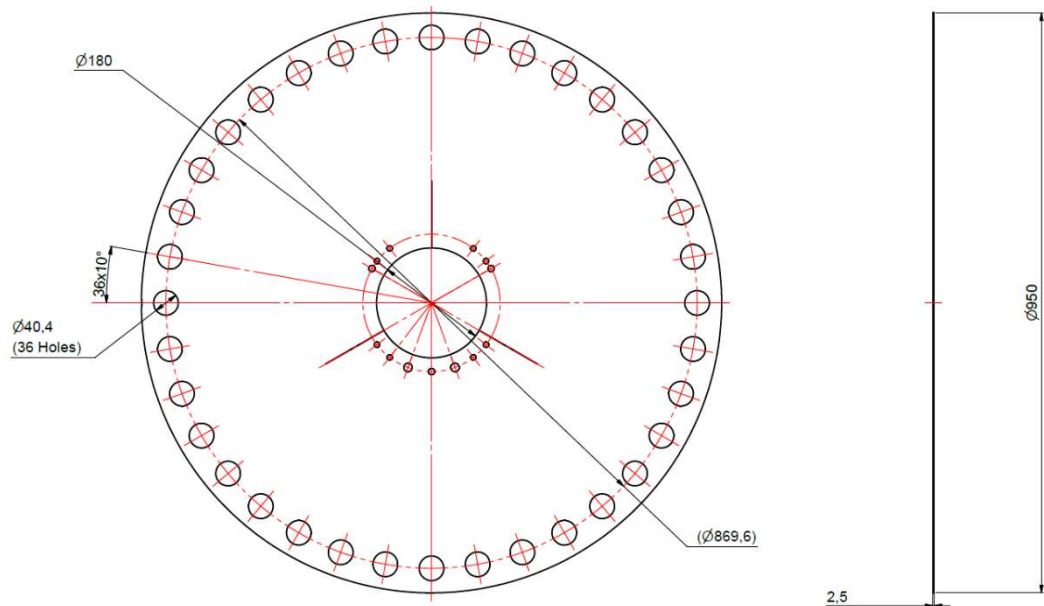


Figure 19. Technical drawing of rotary table for 36 pieces.

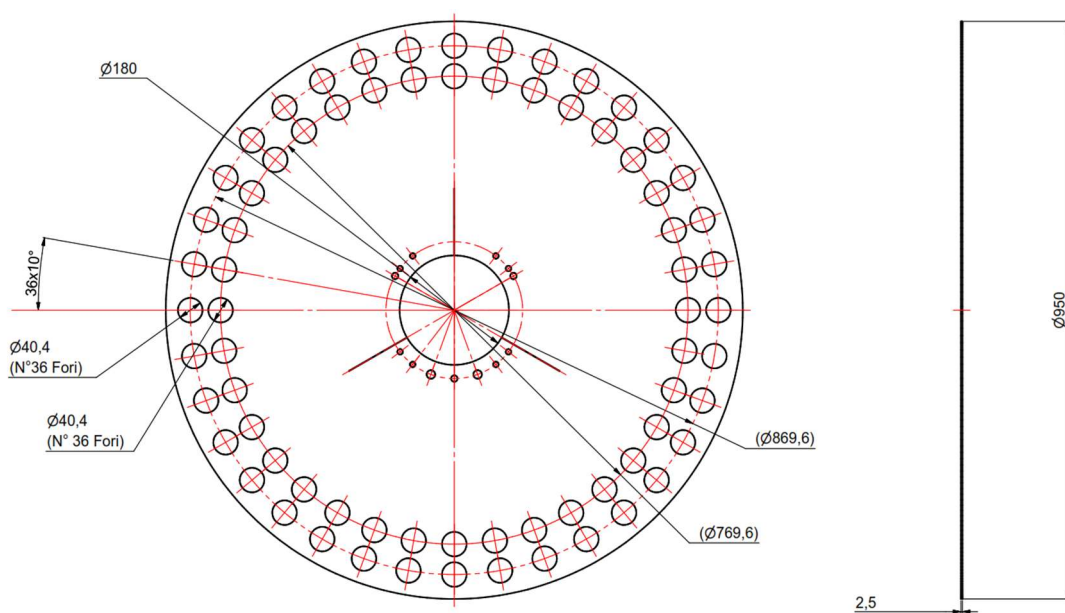


Figure 20. Technical drawing of rotary table for 72 pieces.

5.2. Workpiece Specification

The workpiece that is going to be ground is a ring-shaped disc made of Aluminium Oxide (Al_2O_3) with outer diameter of around 39 mm and inner diameter of 22.7 mm. The thickness

of the original workpiece is around 4.4 mm, with a “step” of around 2.2 mm towards the inner diameter of the workpiece. Figure 21 represents all dimensions of the workpiece.

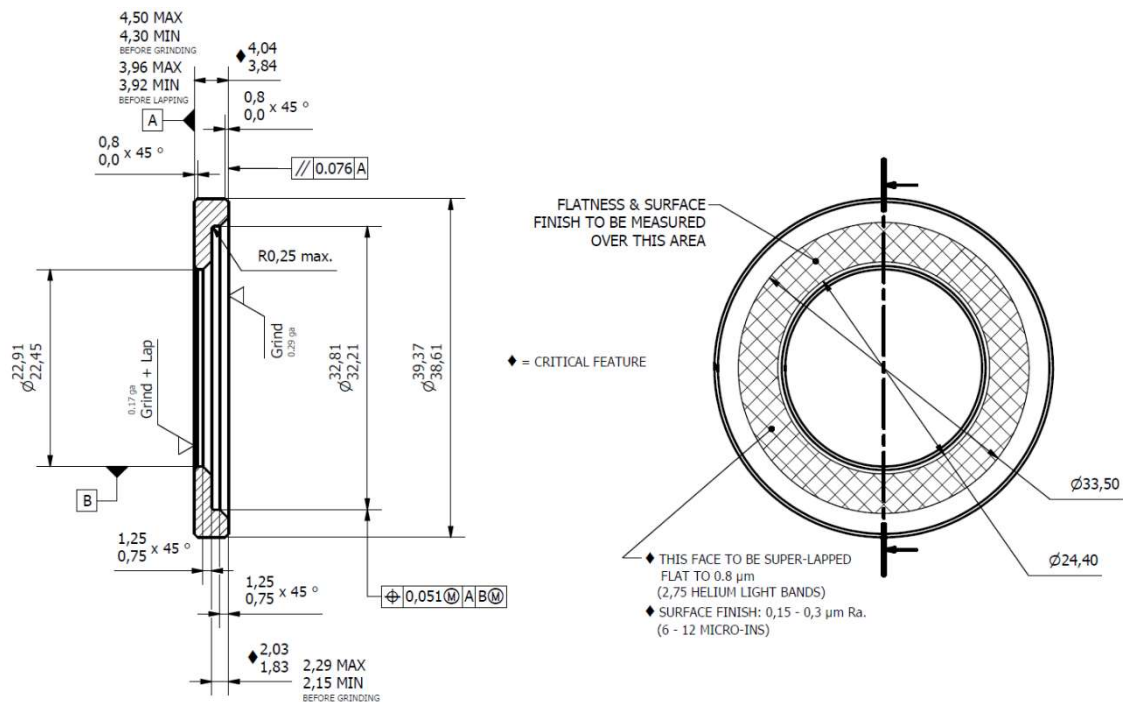


Figure 21. Technical drawing of the specimen.

5.3. Grinding Wheel Specification

The grinding wheel specification used during the test is K-DIA 113 D54 C50 which is supplied by *Diamant-Gesellschaft Tesch GmbH*. The choice of the grinding wheel has been specified by the supplier, in which the company sent the grinding process requirements to the supplier, such as the workpiece material (*Alumina*), the dimensions of the workpiece, the stock removal of the workpiece (2 mm for top and bottom side), and the target output of the grinding machine (50 pcs/min). By checking in their catalogue, its characteristics can be obtained (6):

- K-DIA 113 = Resin-diamond bond for wet or dry grinding with low grinding force.
- D54 = Size of diamond grit based on FEPA Standard; average grit size of 0.045 mm.
- C50 = Concentration of diamond in the rim; 2.2 carats per cm³.

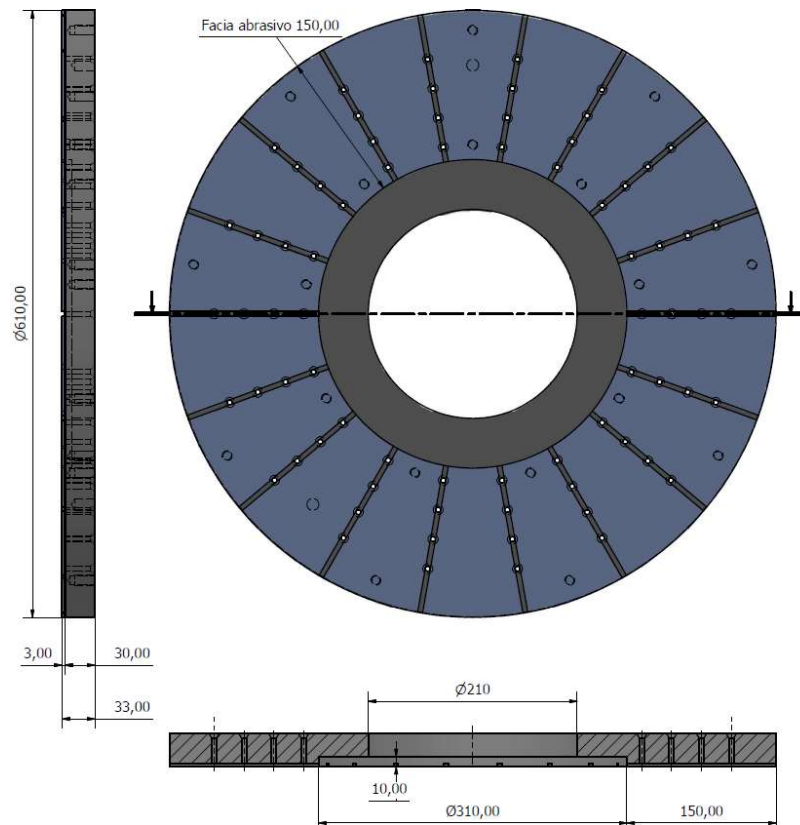


Figure 22. Technical drawing of the grinding wheel.

The type of grinding wheels used is *6A2 Double Side Face Grinding* according to FEPA Standard, with the dimension of 610 mm in diameter, 150 mm of abrasive band with 3 mm of abrasive thickness, and the overall thickness of 33 mm including the core, as shown in Figure 22.

5.4. Grinding Requirements

The customer demanded to machine the top and bottom surface of the specimen from the original thickness of 4.3-4.5 mm to 3.92-3.96 mm. Another critical feature is to obtain the thickness of the “step” from 2.15-2.29 mm before machining to 1.83-2.03 mm after machining. The surface finish of the bottom surface must be between 0.15 to 0.3 μm Ra, while its flatness must be around 0.8 μm after lapping process (during the test, the lapping process is not considered and the upper specification limit of 5 μm is set for the flatness after grinding). Based on the shaded area from the technical drawing in Figure 21, the flatness of the surface is measured on two different diameters: the internal diameter (25 mm) and the external diameter (32 mm). The stock removal of the workpiece in total is 0.4 mm, divided into 0.2 mm for both top and bottom surface.

5.5. Dressing Tool Specification

The dressing tool used is made of white corundum, which mainly consists of *iron-free aluminium oxide* (Al_2O_3). This type of material is very strong but brittle and thus allows for good self-healing of the dressing tool. Figure 23 shows the dressing tool used for the test.

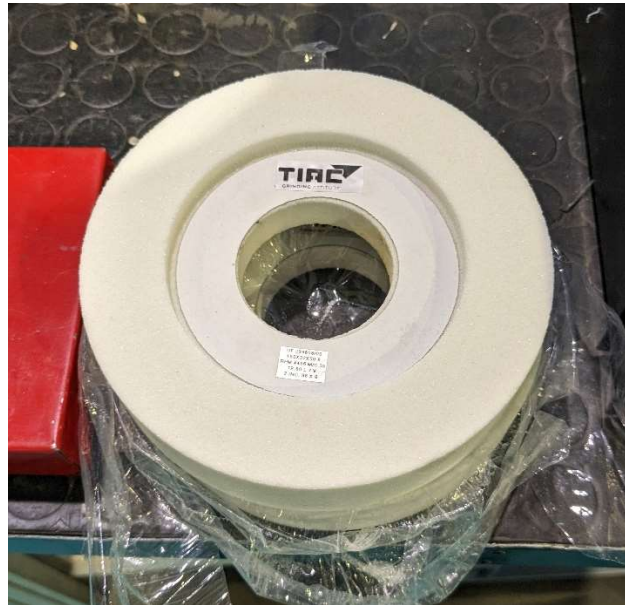


Figure 23. White corundum dressing tool.

The dressing tool for this machine is located in between the two grinding wheels with cross-axis traverse configuration, where the axis of the dresser is orientated at 90° to the wheel axis, as shown in Figure 24. This configuration is able to dress both grinding wheels at the same time.

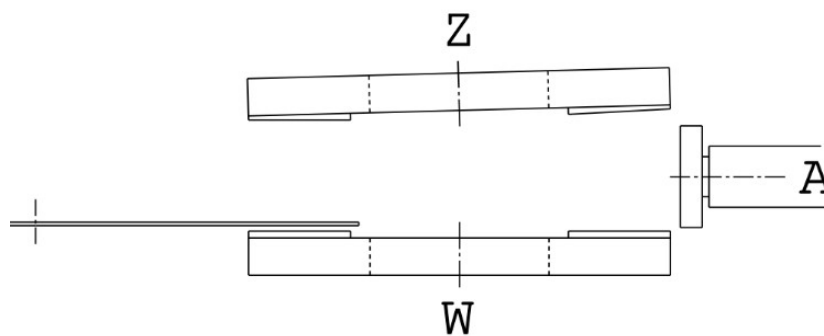


Figure 24. Cross-axis traverse dressing configuration (Z: Top grinding wheel, W: Bottom grinding wheel, A: Dressing tool).

6. Mechanics of Self Rotating Double-Disc Grinding Process

The correlation between the self-rotating movement of the workpiece and its relative placement to the grinding wheel has been studied in (7). There are three classifications of double-disc grinders according to Shanbhag et. al. (8), which are linear through-feed, rotary through-feed, and oscillating. The workpiece traverses through the grinding wheels in all three configurations. As the workpiece traverses through the grinding wheels, it may or may not rotate depending on the moment acting on the workpiece. The study by Dražumerič et. al. (7) has been done on a double-disc grinding machine where the workpiece is placed in a fixed, non-traversing bushing of an index carrier, as shown in Figure 25. When the workpiece faces are not fully covered by the wheel during the grinding process, non-uniform grinding shear forces are present on the workpiece surface, and consequently, a moment acting to force the workpiece to self-rotate within the carrier. The rotation's angular frequency is crucial in this scenario. Excessive heat generation because of high frictional forces can occur if the angular frequency is too high, causing in thermal damage to the bushing. If the angular speed is too low, there is a risk of the workpiece to stop rotating, causing in irregular grinding result on the workpiece.

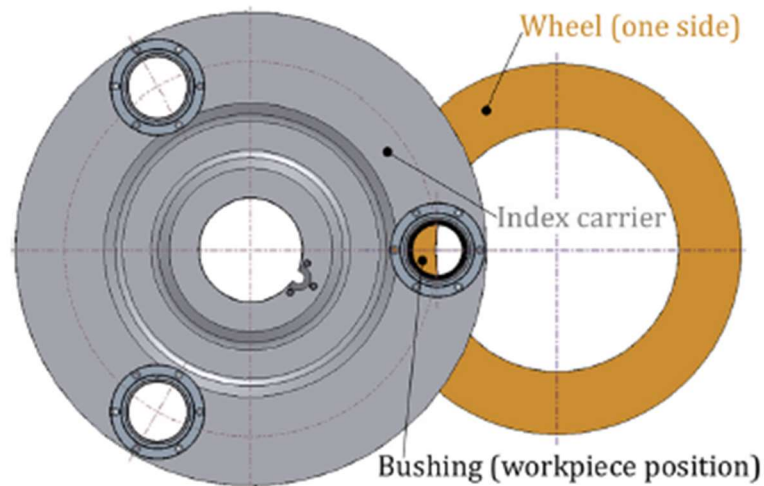


Figure 25. Schematic of index-carrier setup for double-disc grinding (7).

Workpiece coverage ratio (WCR) is the most influential input parameter in defining the process geometry. WCR can be expressed as (7):

$$WCR = \frac{\Delta_0 + r_w}{2r_w}$$

Where Δ_0 is the workpiece-centre position with respect to the grinding wheel radius, r_s , and r_w is the workpiece radius, as shown in Figure 26 (a). WCR = 0 means no wheel-workpiece contact, while WCR = 1 means the entire workpiece is in contact with the wheel. High WCR results in low workpiece angular frequency, ω_w , which can cause workpiece stoppage. On the other hand, low WCR causes high workpiece angular frequency that can lead to greater frictional heat generation at workpiece-bushing interface and greater bushing wear.

The workpiece is held in the radial direction only, which enables it to move in the axial direction freely. The fixed plunge feed rate, v_f , of the closing of the wheels will cause two different feedrates, v_{f1} and v_{f2} , as the effect of different dimples radii (r_{d1} and r_{d2}) of the top and bottom sides of the workpiece, as shown in Figure 26 (b).

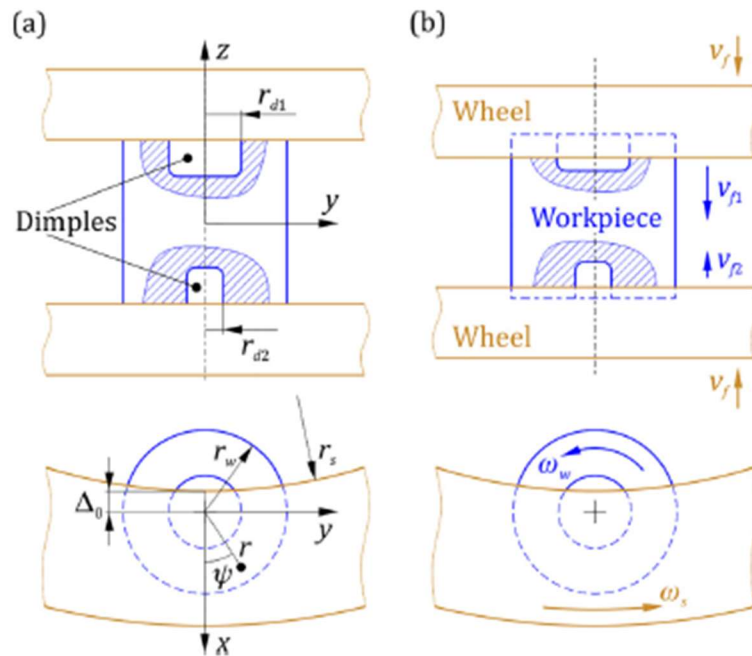


Figure 26. (a) Geometry and (b) kinematics of double disc grinding process (7).

Figure 27 illustrates the distribution of moment on the wheel-workpiece contact patch. The contact patch consists of mostly the workpiece face portion, S_{face} , and the minor side-plunge portion, S_{plunge} , according to: $S_c = S_{face} + S_{plunge}$.

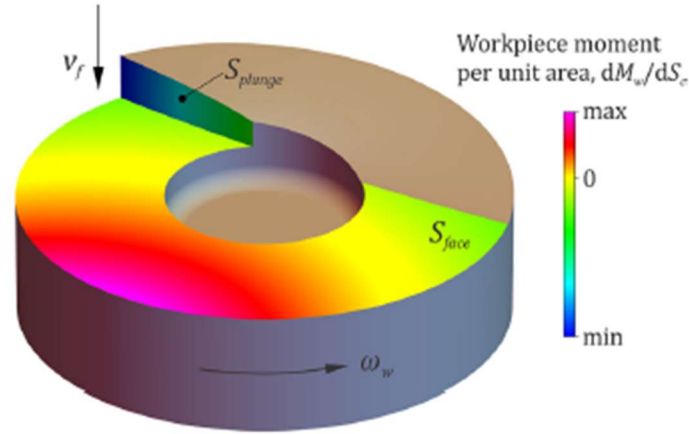


Figure 27. Illustration of workpiece-moment distribution on the wheel-workpiece contact patch (7).

The experiment is done using Lidköping DG300 double-disc face-grinding machine with two resin-bonded Al_2O_3 grinding wheels (diameter 300 mm). The workpiece is bearing cylindrical rollers made from 100CrMnSi6-4 steel. There are two workpiece geometries to be considered: Roller A ($r_w = 15$ mm, $r_{d1} = 1.5$ mm, $r_{d2} = 6$ mm) positioned at WCR = 0.65, and Roller B ($r_w = 15$ mm, $r_{d1} = 8.5$ mm, $r_{d2} = 6$ mm) positioned at WCR = 0.7.

The material removal rate can be determined as (7):

$$Q_w = \iint_{S_c} \vec{v} \cdot \vec{n} dS = \pi(r_w^2 - r_{d1,2}^2)v_{f1,2}$$

Figure 28 shows the material removal rate between the side-plunge portion of the wheel and the wheel face. The difference between the dimple sizes resulting in different feed rates between the top and bottom surface of the workpiece. The material removal rate of the top and bottom surface is also affected by WCR value. As the WCR increases, the material removal rate on the face becomes more dominant. However, the total material removal rate remains about constant regardless of the WCR value.

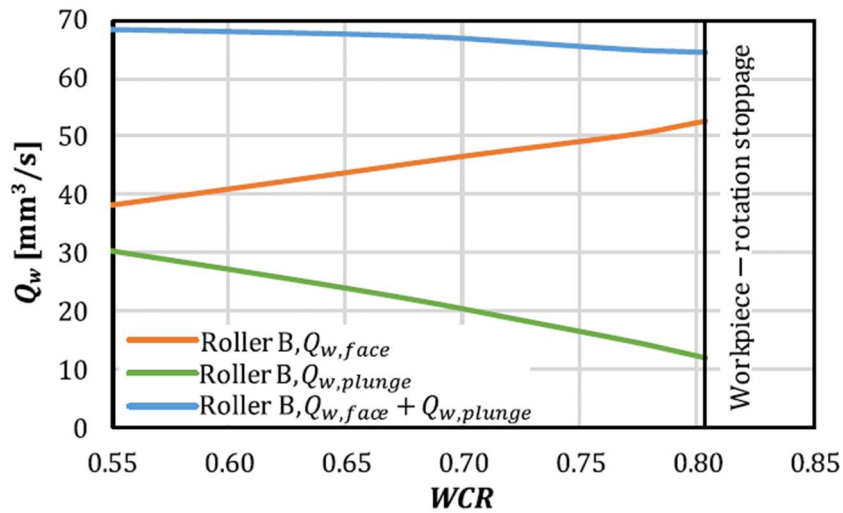


Figure 28. Material removal rate vs. WCR (7).

The predicted value of the angular frequency of the workpiece has been validated by performing direct measurement of acoustic emission (AE) of the frictional contact between the bushing and the workpiece. Dittel 4100-2 process-monitoring system was used to detect the AE energy with Mini-S sensor mounted on the index carrier. The workpiece angular frequency reduces as the WCR and v_f increase until the rotation of the workpiece stops. Dimple size also affects the workpiece rotation. For example, workpiece with full face rotates slower than the workpiece that has a ring-like shape. Figure 29 shows the workpiece angular velocity with different feed rates and WCR values. The measured angular frequency based on AE signals is also included.

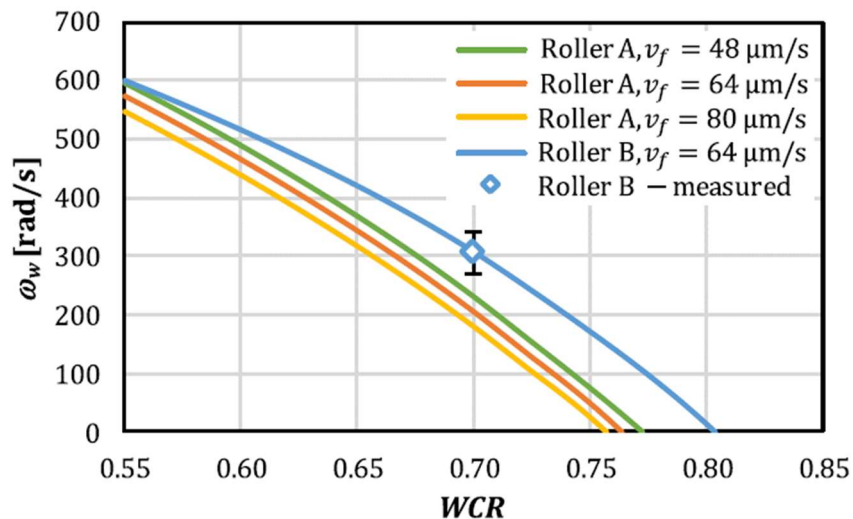


Figure 29. Workpiece angular frequency vs. WCR (7).

In this case study, the safe WCR value is 0.65, which does not cause any excessive heating of the bushing, and the process runs far from the workpiece stoppage threshold ($WCR \approx 0.8$), resulting in consistent grinding operation.

It should be noted that this study has been performed using different machine configurations with different grinding wheels and workpiece dimensions. Another difference is that a bushing has been incorporated into the index carrier to hold the workpiece, whereas the machine used for this thesis places the workpieces loosely fit into the carrier/rotary table.

7. Design of Experiment

On this chapter, the detailed explanation of the experiment procedures, such as the variables of experiment, measuring devices, exporting the data to be analysed, test measurement validation, and the experiment results are presented.

7.1. Flowchart of The Experiment

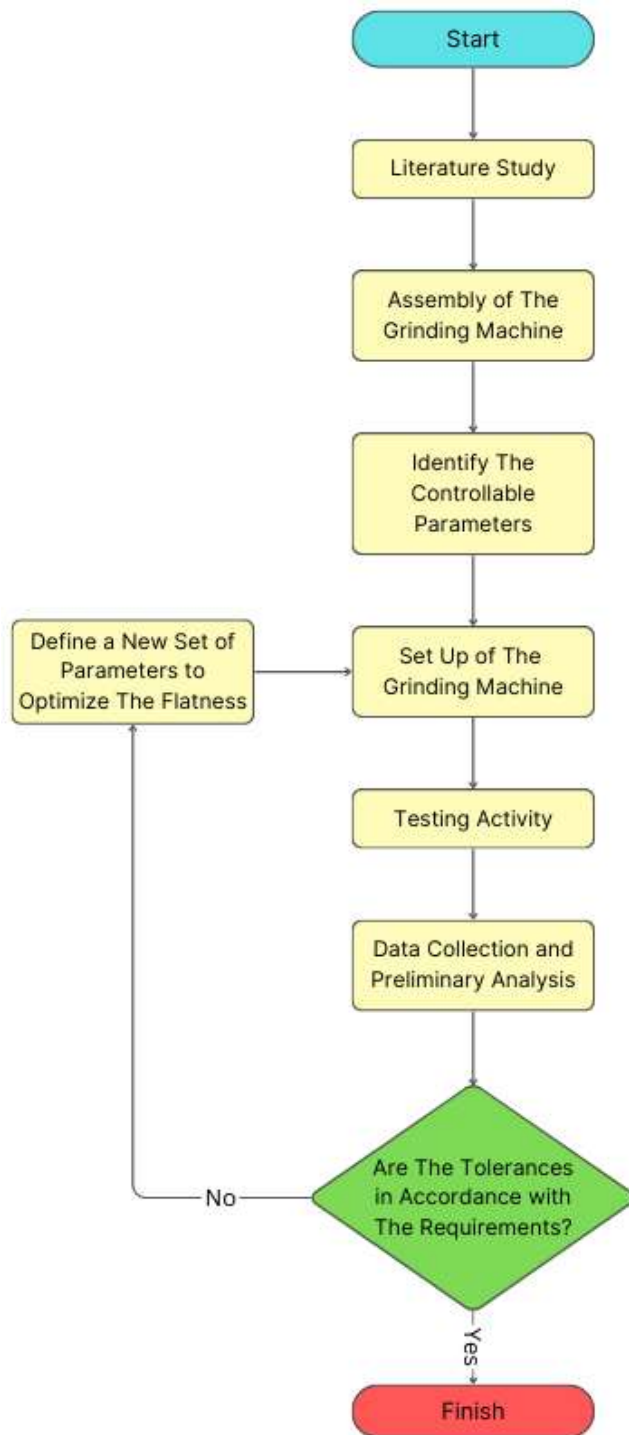


Figure 30. Flowchart of the experiment.

Figure 30 shows the flowchart of the experiment. The experiment starts from literature study about grinding operation, specifically for vertical axis double disc grinders. Then, the grinding machine is assembled that is specific to the workpiece dimensions and requirements. The next step is to identify the controllable parameters of the grinding machines, and to find the suitable set-up to achieve the best grinding result. Finding the best machine set-up is an iterative cycle where it starts from a baseline parameter, then some samples are produced, and the measurement data are collected to be compared to the workpiece requirements. If the requirements have not been met, a new set of parameters is defined to further optimised the grinding result.

7.2. Main Variables of Double-Disc Grinding Machine

It is important to adjust and set the right parameters of the grinding machine to achieve the desired machining result. In the case of vertical spindle double disc grinding machine with rotary table, the parameters that can be adjusted are grinding wheel openings, grinding wheel speed, and rotary table speed. As for the coolant, the type of the coolant has been chosen by the supplier, which is oil and water-based mixture. The coolant flow has also been determined at 3 L/min by the supplier.

7.2.1. Grinding Wheel Openings

In the *Viotto grinding machine*, it is possible to adjust the inclination of the top grinding wheel. The inclination is crucial in grinding process to ensure the workpiece is ground gradually, utilising the whole abrasive band. Only the inclination of the top grinding wheel can be adjusted, while to bottom grinding wheel is positioned flat with respect to the rotary table. The inclination will determine the openings of the grinding wheel on its longitudinal and transversal axis. There are many variables to determine the inclination of the grinding wheel, such as material stock removal (S , *sovrametallo*), distance between the grinding wheel axis and the rotary table axis (I , *interasse*), diameter of the workpiece (D_E , *diametro pezzo*), diameter of the grinding wheel (D_M , *diametro mola*), abrasive band (F , *fascia mola*), and the workpiece-centre position with respect to the grinding wheel radius, or the overhang (Δ_0 , *sporgenza*).

First, it is necessary to find the pitch radius (R_P , *raggio primitivo*), or the radius where the workpieces are placed on the rotary table.

$$R_P = I - R_M + F + \Delta_0 - R_E$$

Where R_M and R_E are radius of grinding wheel and radius of workpiece, respectively. The overhang of the workpiece of $\Delta_0 = 5 \text{ mm}$ has been chosen by the company's engineer, which gave the WCR value of 0.876. This WCR value is rather high in comparison to the study of (7). However, the small overhang value has been chosen in order for the workpiece to not fall off the rotary table.

$$R_p = 605 - 305 + 150 + 5 - 20.2$$

$$R_p = 434.8 \text{ mm}$$

After the pitch radius is found, a diagram can be drawn to determine the opening geometries, as shown in Figure 31.

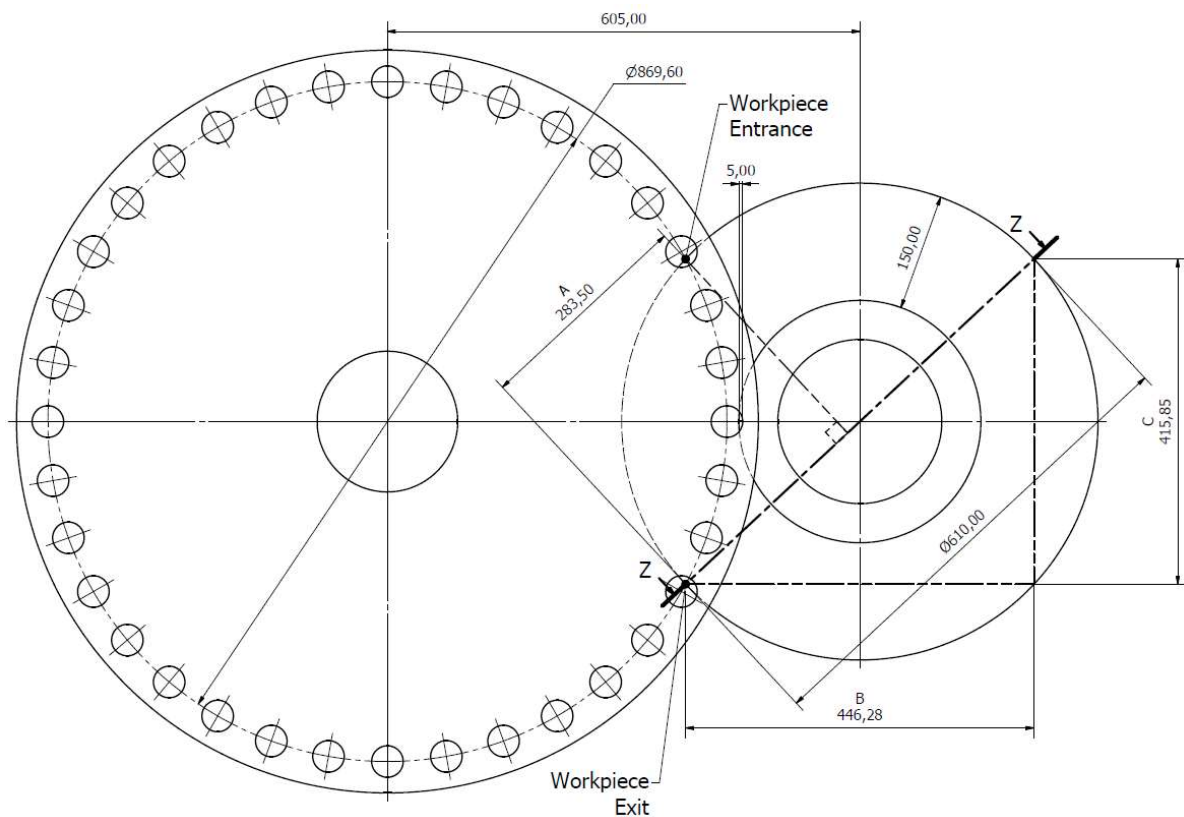


Figure 31. Rotary table-grinding wheel geometry diagram.

By using this diagram, it is possible to define the dimensions of line A, B, and C to determine the grinding wheel openings:

$$A = 283.5 \text{ mm}$$

$$B = 446.28 \text{ mm}$$

$$C = 415.85 \text{ mm}$$

Line A represents the projected distance that the workpiece must travel from the entrance to the exit of the grinding wheel opening. Whereas Line B and C are the projected total

opening line to both longitudinal and transversal axis of the grinding wheel, respectively. Then, the cross-section Z-Z is used to determine the total opening (AP_{TOT} , *apertura totale*) as shown on Figure 32.

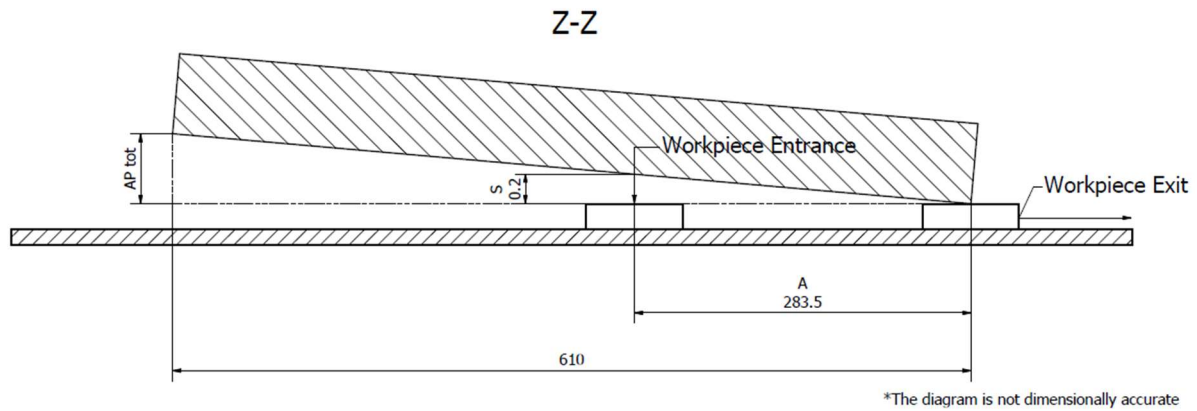


Figure 32. Diagram for total opening of the top grinding wheel.

By setting the stock removal $S = 0.2 \text{ mm}$, it is possible to define the AP_{TOT} with simple geometry.

$$\frac{S}{A} = \frac{AP_{TOT}}{D_M}$$

$$AP_{TOT} = \frac{S \cdot D_M}{A}$$

$$AP_{TOT} = \frac{0.2 \cdot 610}{283.5} = 0.43 \text{ mm}$$

The same formula is used to define the longitudinal and transversal openings using dimension of B and C, respectively.

- Longitudinal opening:

$$\frac{AP_{LONG}}{B} = \frac{AP_{TOT}}{D_M}$$

$$AP_{LONG} = \frac{AP_{TOT} \cdot B}{D_M}$$

$$AP_{LONG} = \frac{0.43 \cdot 446.28}{610} = 0.31 \text{ mm}$$

- Transversal opening:

$$\frac{AP_{TRAS}}{C} = \frac{AP_{TOT}}{D_M}$$

$$AP_{TRAS} = \frac{AP_{TOT} \cdot C}{D_M}$$

$$AP_{TRAS} = \frac{0.43 \cdot 415.85}{610} = 0.29 \text{ mm}$$

After the opening values are found, the grinding wheel openings can be set up using a special aligning tool, as seen on Figure 33.

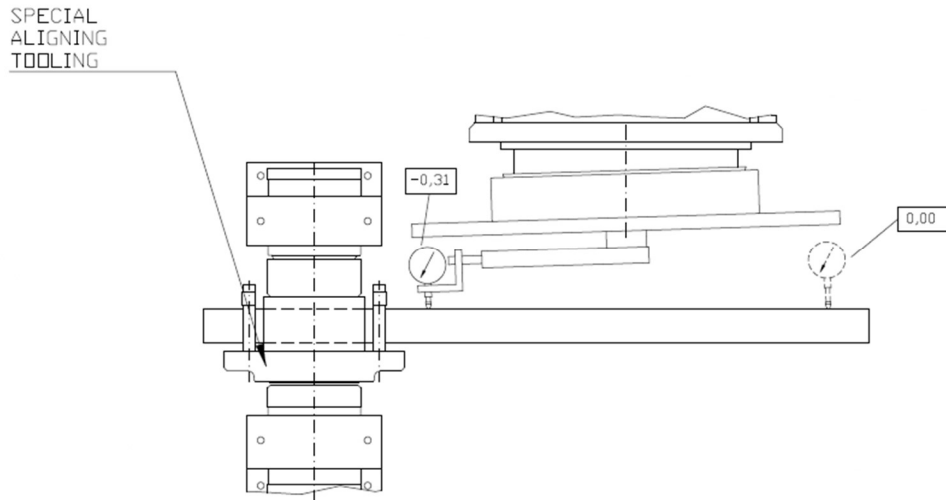


Figure 33. Setting the inclination of the grinding wheel.

This set up is done both for the longitudinal and transversal axis of the grinding wheel, as illustrated by the Figure 34.

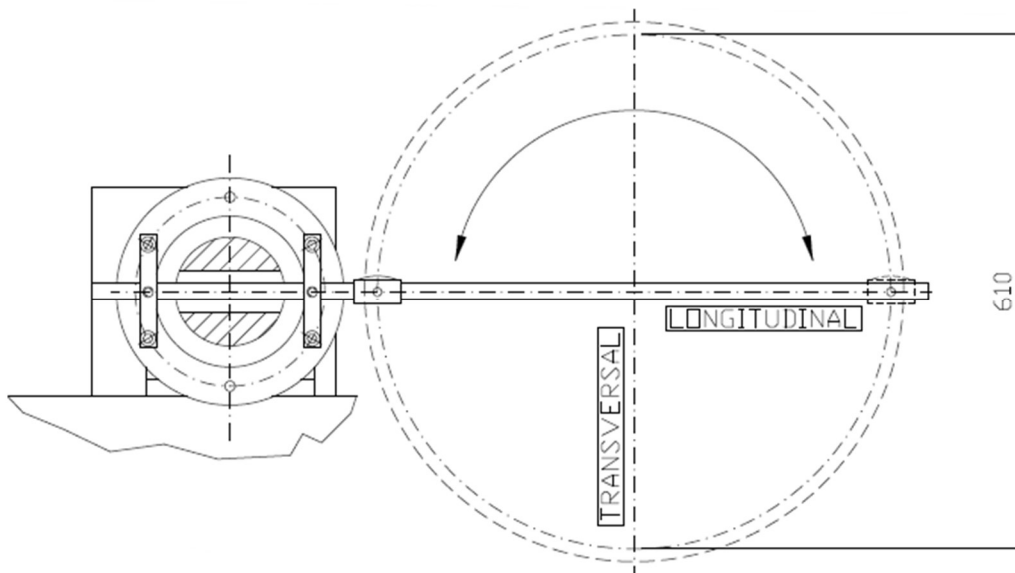


Figure 34. Longitudinal and transversal axes of the grinding wheel.

Different grinding wheel openings are also proposed by manually placing the workpiece in between the grinding wheels on the entrance and exit position of the workpiece path and measure the distance needed for the openings of the top grinding wheel. Using the manual

method, modified grinding wheel openings of 0.21 mm for the longitudinal axis and 0.19 mm for the transversal axis have been found.

7.2.2. Grinding Wheel Speed

The speed of top and bottom grinding wheels can be adjusted separately, depending on the surface area of the workpiece. High grinding wheel speed will result in higher material stock removal, which better suited for bigger workpiece surface area, while the opposite is true for low grinding wheel speed. In this case, the workpiece position is in such a way that the bigger surface area is on the bottom side, thus the bottom grinding wheel is set to have higher speed than the top one. Three sets of grinding wheel speed have been defined during the testing: 300/750 rpm, 400/1200 rpm, and 200/1200 rpm.

7.2.3. Rotary Table Speed

It is possible to adjust the speed of the rotary table in order to modify the production rate. By adjusting the rotary table speed, it is possible to fine tune the material stock removal rate to achieve the desired results. During the testing, two different rotary table speed have been set, based on the production rate of the machine: 45 pcs/min = 1.25 rpm, and 60 pcs/min = 1.66 rpm.

7.3. Variables of Experiment

The measurement procedure is to check the flatness of the workpiece as the priority, and then use the set of parameters that yield the best flatness to check the rest of the workpiece specifications e.g., surface finish, parallelism, thickness, and step thickness.

Table 2. Set of parameters for experiment.

Set of Parameters	Openings	Top Wheel RPM	Bottom Wheel RPM	Wheel Speed Ratio	Rotary Table RPM
1	Original (0.31 mm / 0.29 mm)	400	1200	3.0	1.25 (45 pcs/min)
2	Original (0.31 mm / 0.29 mm)	400	1200	3.0	1.66 (60 pcs/min)
3	Modified (0.21 mm / 0.19 mm)	300	750	2.5	1.66 (60 pcs/min)

4	Modified (0.21 mm / 0.19 mm)	120	1200	10.0	1.66 (60 pcs/min)
---	---------------------------------	-----	------	------	-------------------

The choice of value for each parameter are defined by the experience of the machine operator. The parameters set #1 and #2 represent the grinding wheels speed ratio of 3. The parameters set #3 represent the baseline setup for the grinding machine with speed ratio of 2.5. And the parameters set #4 represent the top and bottom grinding wheels speed ratio of 10.

The speed ratio between the top and bottom grinding wheels an important factor in double disc grinding machine because it affects how much stock removal of the top and bottom surface of the workpiece. Because of the position of workpiece during the grinding, the bottom grinding wheel needs to rotates faster than the top one in order to achieve the desired stock removal.

7.4. Measuring Devices

After the workpiece has been ground, its dimensions were checked and compared them with the customer's specifications. High accuracy measurement devices are used to check the workpiece dimensions, such as its surface flatness and roughness.

7.4.1. Flatness Measurement

The surface flatness of the workpiece is measured around the defined area using roundness tester with turntable. The workpiece is placed on the centre of the turntable, the turntable spins the workpiece, and a measuring probe is place on top of the workpiece surface to achieve continuous measurement along a given circumference. By using this technique, it is possible to have a full 360 degrees of measurement of the surface flatness. During this experiment, the flatness measurement is done on the internal and external flatness. The internal flatness corresponds to the surface flatness of the top side of the workpiece, in which the measurement has been done at a diameter of 25 mm of the workpiece surface. The external flatness refers to the measurement at a diameter of 32 mm of the workpiece surface.



Figure 35. Mitutoyo Roundtest RA-2200 roundness tester.

7.4.2. Roughness Measurement

A portable handheld surface roughness tester is used to measure the surface roughness. This device measures the roughness of a surface by using a probe which is placed on top of the surface and moves the probe along the surface to calculate its roughness. The device will automatically calculate the average roughness (Ra) of the surface.



Figure 36. TESA 06930015 TWIN-SURF portable roughness tester.

7.4.3. Dial Indicator

Dial Indicator with granite plate is used when fast and accurate measurement is needed. The problem with flatness measurement like CMM or roundness tester is that it takes some time to operate. Dial indicator can be used on the shop floor with ease and provides decent accuracy to measure the thickness of the workpiece.



Figure 37. Dial Indicator.

7.5. Exporting the Data for Analysis

The workpiece that has been ground is then measured on the roundness tester for its flatness. The measurement output of the roundness tester is printed out in a company-specific report format, and the data from the report are submitted manually into *Microsoft Excel*. Figure 38 is one of the examples of the measurement report from the testing activity.

Data analysis is done using *Minitab* Software. *Minitab* is a data analysis software that is capable of performing various statistical analyses, such as: hypothesis testing, regression analysis, ANOVA, etc. *Minitab* also provides graphical tools for better understanding of the data. The data that has been collected using *Microsoft Excel* can easily be imported to *Minitab* for further analysis.

Vista complessiva				
	A	B	C	D
				0001
	F	0.0032	FLAT_PLA_INT_PZ_1 (PLA_INT_PZ_1) (PLAT)	0.0050
	F	0.0038	FLAT_PLA_EST_PZ_1 (PLA_EST_PZ_1) (PLAT)	0.0050
	F	0.0046	FLAT_PLA_INT_PZ_2 (PLA_INT_PZ_2) (PLAT)	0.0050
	F	0.0050	FLAT_PLA_EST_PZ_2 (PLA_EST_PZ_2) (PLAT)	0.0050
	F	0.0033	FLAT_PLA_INT_PZ_3 (PLA_INT_PZ_3) (PLAT)	0.0050
	F	0.0040	FLAT_PLA_EST_PZ_3 (PLA_EST_PZ_3) (PLAT)	0.0050
	F	0.0040	FLAT_PLA_INT_PZ_4 (PLA_INT_PZ_4) (PLAT)	0.0050
	F	0.0046	FLAT_PLA_EST_PZ_4 (PLA_EST_PZ_4) (PLAT)	0.0050
	F	0.0042	FLAT_PLA_INT_PZ_5 (PLA_INT_PZ_5) (PLAT)	0.0050
	F	0.0025	FLAT_PLA_EST_PZ_5 (PLA_EST_PZ_5) (PLAT)	0.0050
	F	0.0020	FLAT_PLA_INT_PZ_6 (PLA_INT_PZ_6) (PLAT)	0.0050
	F	0.0040	FLAT_PLA_EST_PZ_6 (PLA_EST_PZ_6) (PLAT)	0.0050
	F	0.0033	FLAT_PLA_INT_PZ_7 (PLA_INT_PZ_7) (PLAT)	0.0050
	F	0.0050	FLAT_PLA_EST_PZ_7 (PLA_EST_PZ_7) (PLAT)	0.0050
	F	0.0020	FLAT_PLA_INT_PZ_8 (PLA_INT_PZ_8) (PLAT)	0.0050
	F	0.0032	FLAT_PLA_EST_PZ_8 (PLA_EST_PZ_8) (PLAT)	0.0050
	F	0.0020	FLAT_PLA_INT_PZ_9 (PLA_INT_PZ_9) (PLAT)	0.0050
	F	0.0033	FLAT_PLA_EST_PZ_9 (PLA_EST_PZ_9) (PLAT)	0.0050
	F	0.0023	FLAT_PLA_INT_PZ_10 (PLA_INT_PZ_10) (PLAT)	0.0050
	F	0.0030	FLAT_PLA_EST_PZ_10 (PLA_EST_PZ_10) (PLAT)	0.0050

 VIA DALMAZIA 16 /18 NOVA MILANESE (MB)	Progetto	MISURAZIONI MORGAN	Cliente	MORGAN
	Disegno		Operatore	G.P.
	Numero serie		Firma	
	ID pezzo		Note	PZ DA A 1 A 10
	Modello CAD		Pagina	1 di 1
	Data	06-07-2023		

Figure 38. Measurement report.

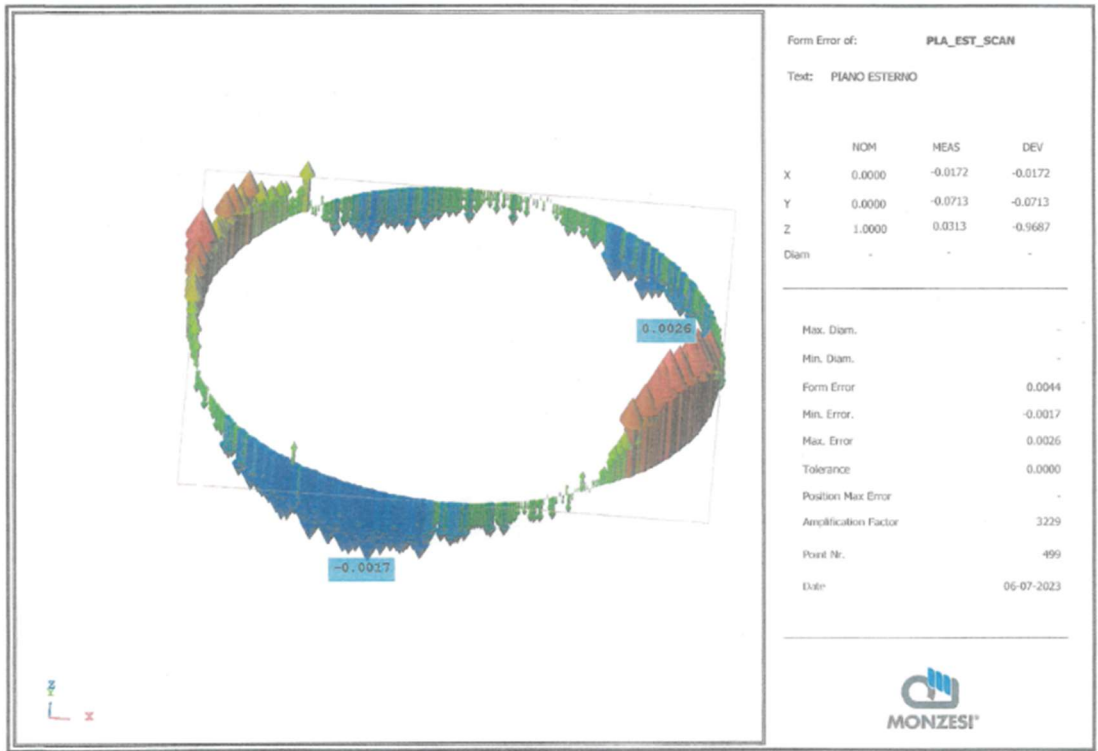


Figure 39. External flatness report.

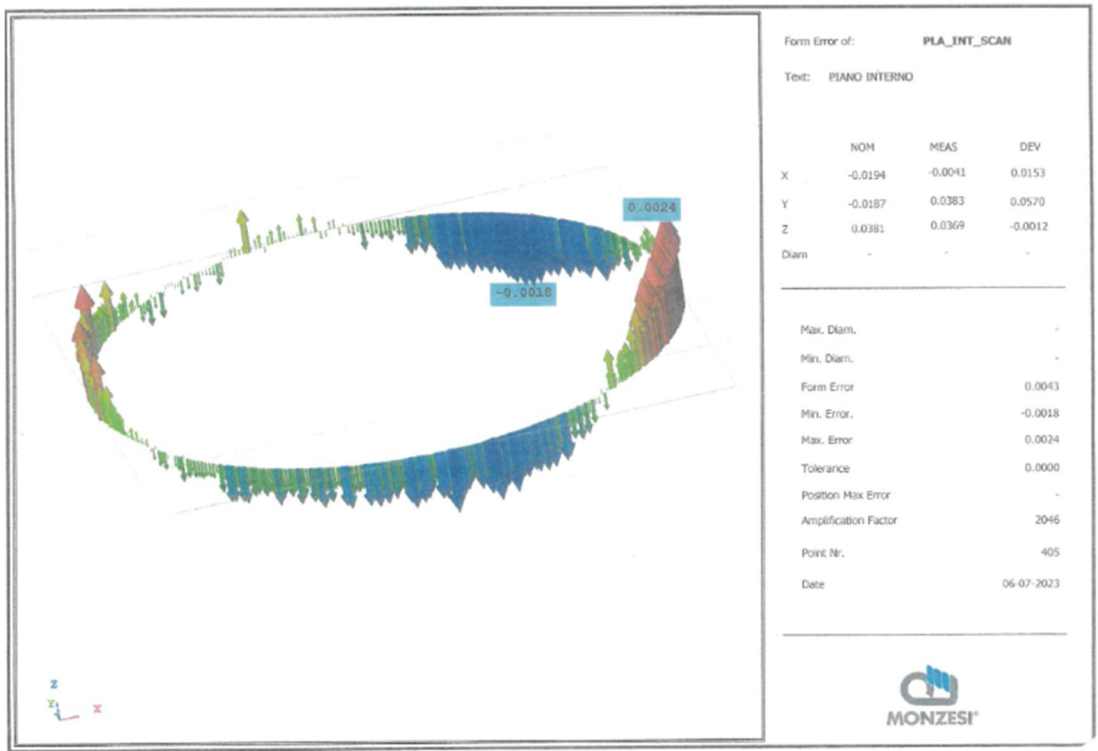


Figure 40. Internal flatness report.

7.6. Test Measurement Validation

It is necessary to crosscheck the measurement result from in-house facility with the result from another third-party measuring company to ensure the integrity of the measurement. The crosscheck is carried out by CPM in which they have done flatness measurement of the workpieces that have been measured by the in-house facility. Figure 41 shows the measurement result done by CPM, and Figure 42 represents the in-house measurement result.

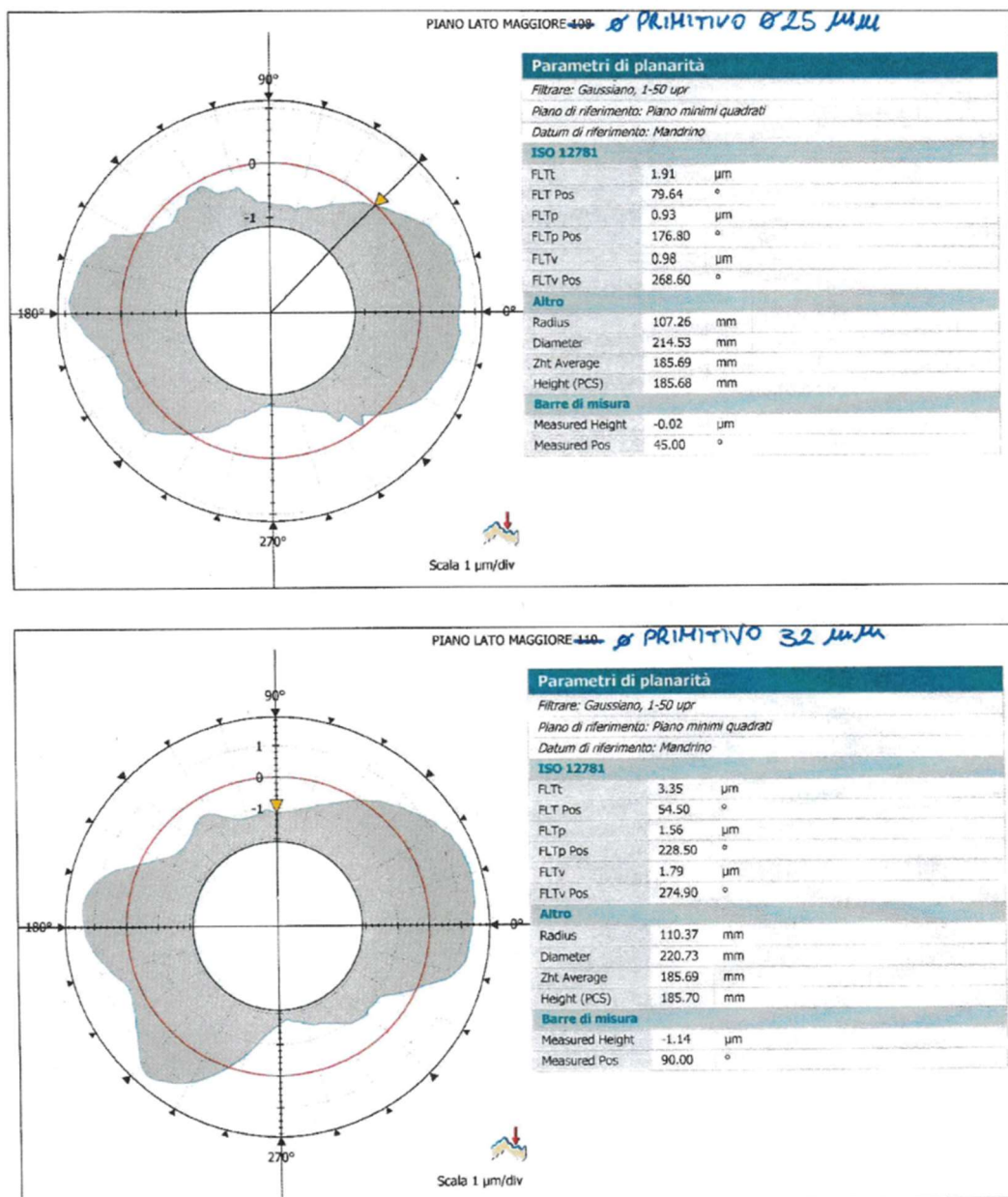


Figure 41. Third-party measurement result.

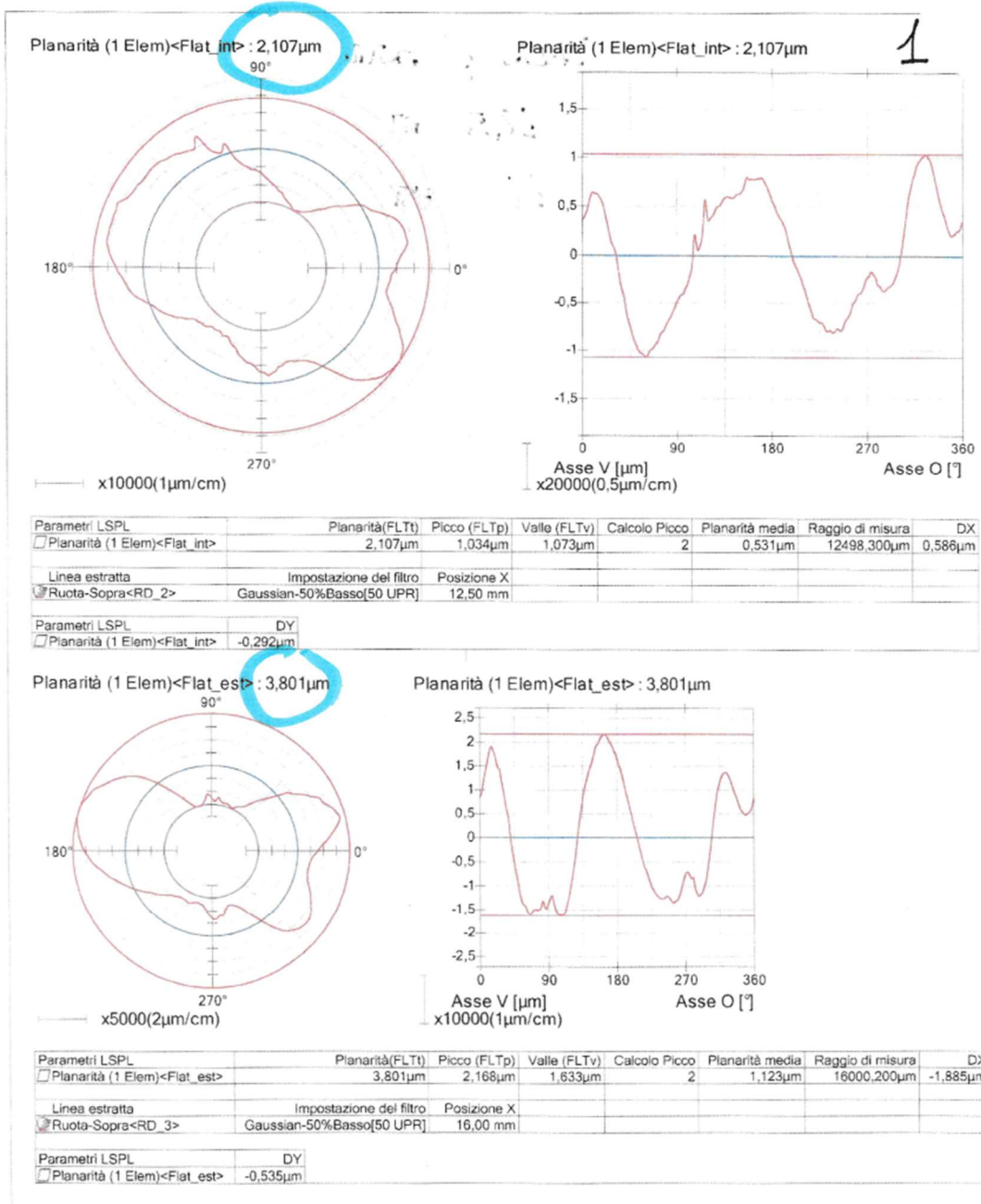


Figure 42. In-house measurement result.

By comparing the results between the in-house facility and the CPM facility, the average differences in flatness for internal diameter and external diameter are around 7.47% and 7.84% respectively, where the measurements of CPM are lower. It is most likely that the measurements done in-house are more conservative compared to the CPM. Even though the differences are quite significant (more than 3%), the difference in absolute value of the measurements are around 0.1-0.4 µm, which are not significant. Thus, the in-house facility is used to measure all the test data.

7.7. Experiment Results

During the testing activity, there are four sets of parameters with different value of openings (modified and original), top wheel RPM (120, 300, and 400 RPM), bottom wheel RPM (750 and 1200 RPM), and rotary table RPM (1.25 and 1.66 RPM). For each dataset, three random samples are chosen for this analysis.

After the analysis has been completed for the flatness, the parameters set that yield the best result is then chosen for the next step of test to evaluate the surface finish, parallelism, thickness, and step dimensions.

Before performing the test with multiple sets of parameters, the first evaluation is to compare the grinding capability of the inner and outer ring of the rotary table. The outcome of this evaluation will determine the processing capacity of the grinding machine.

7.7.1. Comparison between Inner and Outer Ring

The evaluation is performed using baseline parameters:

- Top wheel speed: 300 RPM
- Bottom wheel speed: 750 RPM
- Rotary table speed: 0.85 RPM
- Grinding wheel openings: Original

Table 3 represents some samples of the grinding result performed using both inner and outer ring of the rotary table. Seven samples are taken randomly from 25 pieces that have been tested. The measurement is taken by taking the difference between the required thickness of the workpiece (3.94 mm) and the actual thickness of the workpiece after the grinding process.

Table 3. Difference of workpiece thickness between the inner ring and the outer ring.

#Workpiece	Difference in Thickness to The Requirement	
	Outer Ring (μm)	Inner Ring (μm)
1	3.3	25.3
2	7.1	22.2
3	5.2	20.3
4	10.2	27.7
5	8.4	41.3

6	4.1	58.9
7	4.3	34.1
Average	6.09	32.83
Standard Deviation	2.55	13.58

The result shows that the inner ring of the rotary table gives very bad results in terms of the thickness, with almost four times the difference compared to the outer ring result. With this evaluation, the further tests will be performed only using the outer ring of the rotary table in order to receive more consistent grinding result.

7.7.2. Results of Parameters Set #1 to #4

The grinding result of the parameter #1 to parameter set #4 are shown in Table 4.

Table 4. Grinding result from all set of parameters tested.

Parameters Set	Workpiece	Flatness Internal (μm)	Flatness External (μm)	Average Flatness (μm)
#1	1	4.2	8.7	6.5
	2	5.6	9	7.3
	3	4.6	7.4	6
	Average	4.8	8.4	6.6
#2	1	5.6	8.5	7.1
	2	4.3	6.8	5.6
	3	4.1	14.4	9.3
	Average	4.7	9.9	7.3
#3	1	3.3	3.6	3.5
	2	3.5	4.9	4.2
	3	4.4	4.1	4.3
	Average	3.7	4.2	4
#4	1	2.1	4.2	3.1
	2	3.2	1.5	2.4
	3	2.7	3.8	3.2
	Average	2.7	3.2	2.9

8. Data Analysis

The data that have been collected are then processed using *Minitab* statistical software. This software is able to analyse the distribution of the data and compare one data with another to determine which set of parameters is the most suitable for the grinding process.

8.1. Statistics of The Results

Using *Minitab*, it is possible to easily calculate the mean, standard error of the mean, standard deviation, minimum, and maximum value of each dataset. The analysis of statistics is performed for the internal flatness, external flatness, and average flatness. The average flatness is found by averaging the value of the internal and external flatness.

8.1.1. Statistics for Internal Flatness

Table 5. Statistics for internal flatness.

Variable	Set of Parameters	Total Count	Mean	SE Mean	StDev	Minimum	Maximum
Flatness Int	1	3	4.800	0.416	0.721	4.200	5.600
	2	3	4.667	0.470	0.814	4.100	5.600
	3	3	3.733	0.338	0.586	3.300	4.400
	4	3	2.667	0.318	0.551	2.100	3.200

By looking at the data, the parameters set #4 has the lowest mean value of 2.667 μm , followed by parameters set #3, #2, and #1. The parameters set #4 also has the lowest standard deviation of 0.551.

8.1.2. Statistics for External Flatness

Table 6. Statistics for external flatness.

Variable	Set of Parameters	Total Count	Mean	SE Mean	StDev	Minimum	Maximum
Flatness Ext	1	3	8.367	0.491	0.850	7.400	9.000
	2	3	9.90	2.30	3.99	6.80	14.40
	3	3	4.200	0.379	0.656	3.600	4.900
	4	3	3.167	0.841	1.457	1.500	4.200

By looking at the data, the parameters set #4 has the lowest mean value of 3.167 μm , followed by parameters set #3, #1, and #2. However, the parameters set #3 has the lowest standard deviation of 0.656.

8.2. One-way ANOVA

ANOVA (analysis of variance) is one of the most common methods used in statistical analysis to test the hypothesis. Hypothesis tests include two hypotheses (claims), the null hypothesis (H_0) and the alternative hypothesis (H_1). The null hypothesis is the initial claim and is often specified based on previous research or common knowledge, whereas the alternative hypothesis is what actually might be true (9). To verify the difference in flatness, a *one-way ANOVA* has been performed, which tests the equality of all four dataset's means. *Tukey's multiple comparison test* has also been performed to see which flatness means are different.

8.2.1. ANOVA of Internal Flatness

Method

Null hypothesis All means are equal
 Alternative hypothesis Not all means are equal
 Significance level $\alpha = 0.05$

Equal variances were assumed for the analysis.

Factor Information

Factor	Levels	Values
Set of Parameters	4	1, 2, 3, 4

Analysis of Variance

Source	DF	Adj SS	Adj MS	F-Value	P-Value
Set of Parameters	3	8.787	2.9289	6.40	0.016
Error	8	3.660	0.4575		
Total	11	12.447			

Model Summary

S	R-sq	R-sq(adj)	R-sq(pred)
0.676387	70.59%	59.57%	33.84%

Means

Set of Parameters	N	Mean	StDev	95% CI
1	3	4.800	0.721	(3.899, 5.701)
2	3	4.667	0.814	(3.766, 5.567)
3	3	3.733	0.586	(2.833, 4.634)
4	3	2.667	0.551	(1.766, 3.567)

Pooled StDev = 0.676387

Grouping Information Using the Tukey Method and 95% Confidence

Set of Parameters	N	Mean	Grouping
1	3	4.800	A
2	3	4.667	A

3	3	3.733	A	B
4	3	2.667		B

Means that do not share a letter are significantly different.

The calculated *P-Value* of the data is much lower than the significance level that has been set ($0.016 < 0.05$) which means that the data is significantly different between each other. On the *Tukey Pairwise Comparisons*, there are two groups of data (A and B) that showcase how significant the difference between set of parameters. The parameters set #1, #2, and #3 can be represented as Group A, whereas parameters set #3 and #4 can be represented as Group B. Interesting to note that the parameters set #3 can be represented both in Group A and B simultaneously.

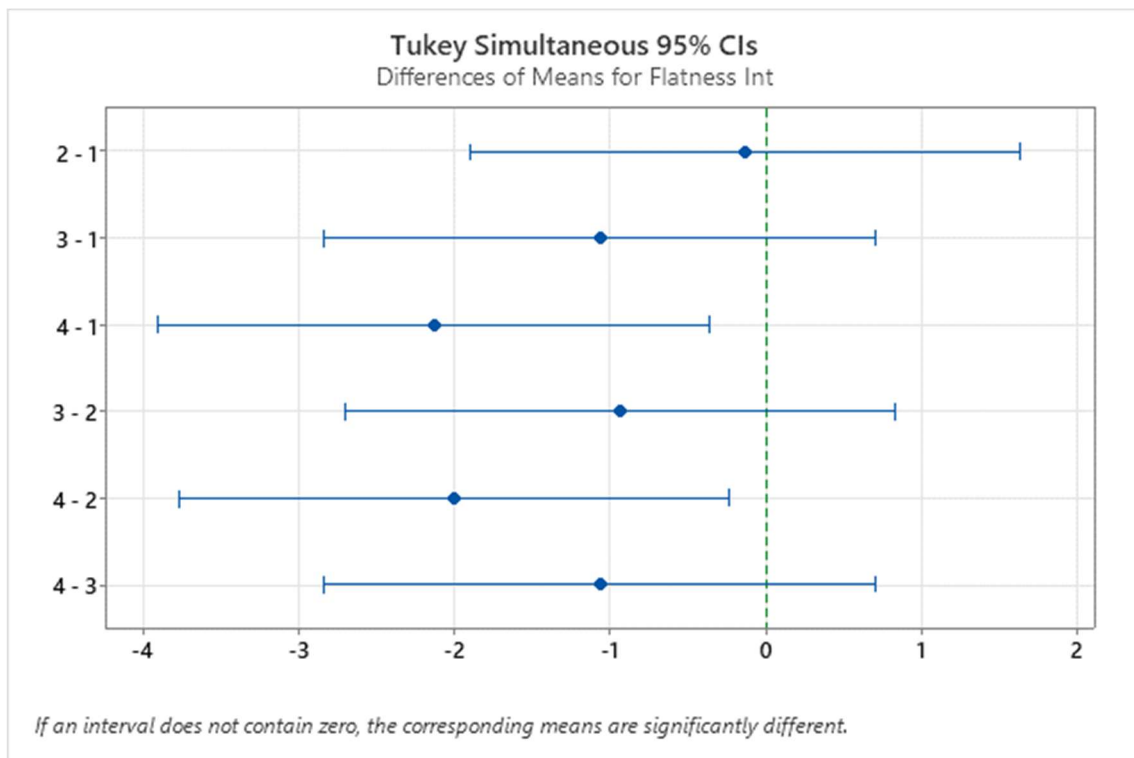


Figure 43. Differences of means of internal flatness.

Figure 43 shows the difference of means for internal flatness between each set of parameters. The line represents the range in which the difference between the data can be found. Whenever the line crosses zero, that means there is a probability that the data may have the same mean values. Parameters set #1 and #2 have the closest correlation between them, whereas parameters set #1 & #4, and #2 & #4 are significantly different. There

is an interesting observation in which parameters set #3 has some correlation with all other datasets.

Figure 44 shows the interval plot of internal flatness for each set of parameters and the mean comparison between them. By using 95% *Confidence Interval*, the probability of the population mean may be found within the interval. The graph shows that there are overlaps between the interval of parameters set #3 with other datasets, which explains the correlation of parameters set #3 from the *Tukey comparisons* chart.

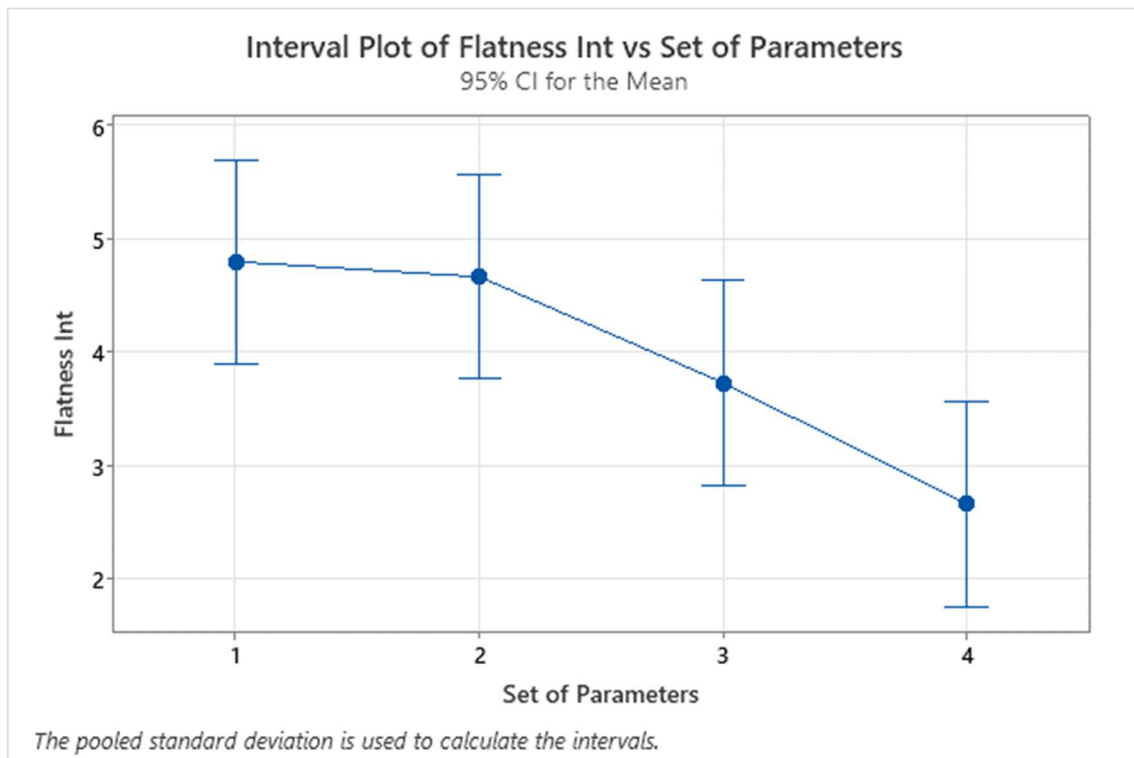


Figure 44. Interval plot of internal flatness.

Figure 45 show the boxplot for each dataset, which also explain the range of value from the minimum to the maximum. The taller the box is, the more spread the data, or it can be said that the data has higher standard deviation value. The parameters set #4 has the lowest average value of internal flatness compared to the other data.

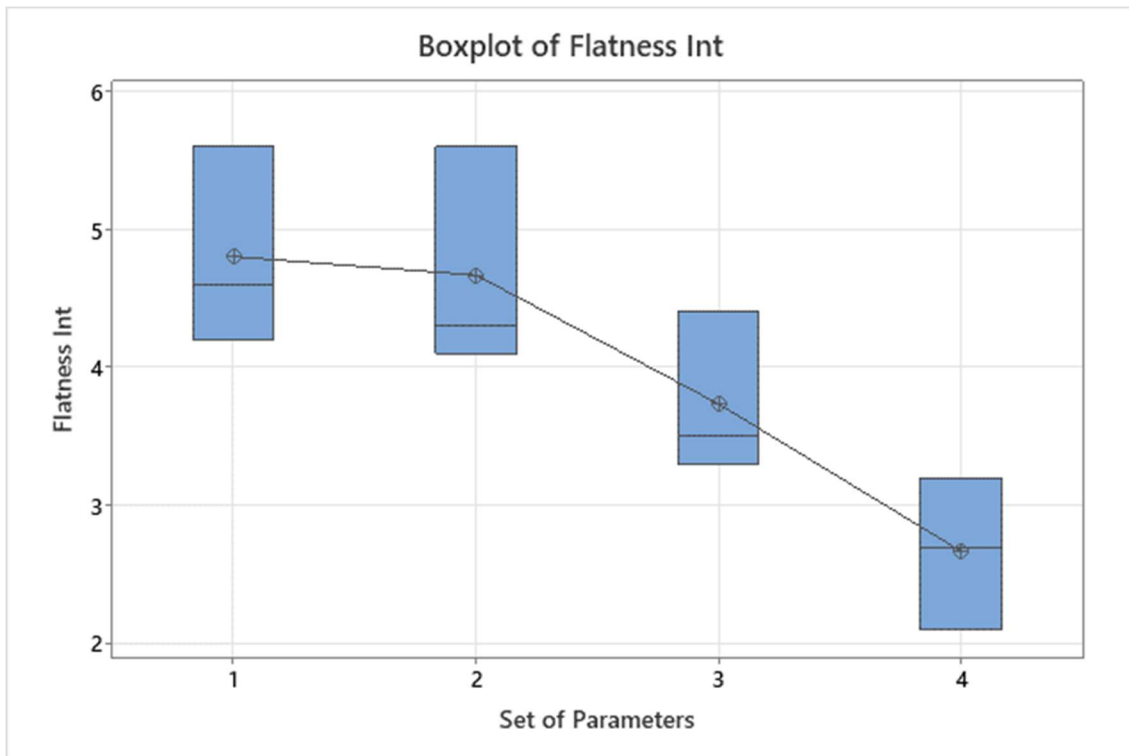


Figure 45. Boxplot of internal flatness.

8.2.2. ANOVA of External Flatness

Method

Null hypothesis: All means are equal
 Alternative hypothesis: Not all means are equal
 Significance level: $\alpha = 0.05$

Equal variances were assumed for the analysis.

Factor Information

Factor	Levels	Values
Set of Parameters	4	1, 2, 3, 4

Analysis of Variance

Source	DF	Adj SS	Adj MS	F-Value	P-Value
Set of Parameters	3	3	54.938	18.313	16.03
Error	8	7	7.998	1.143	
Total	11	10	62.936		

Model Summary

S	R-sq	R-sq(adj)	R-sq(pred)
1.06893	87.29%	81.84%	67.39%

Means

Set of Parameters	N	Mean	StDev	95% CI
1	3	8.367	0.850	(5.451, 11.283)
2	3	7.650	1.202	(5.863, 9.437)
3	3	4.200	0.656	(1.284, 7.116)
4	3	3.167	1.457	(0.251, 6.083)

Pooled StDev = 1.06893

Grouping Information Using the Tukey Method and 95% Confidence

Set of Parameters	N	Mean	Grouping
2	3	9.90	A
1	3	7.650	A

3	3	4.200	A	B
4	3	3.167		B

Means that do not share a letter are significantly different.

The calculated *P-Value* of the data is much lower than the significance level that has been set ($0.015 < 0.05$) which means that the data is significantly different between each other. The parameters set #1, #2, and #3 can be represented as Group A, whereas parameters set #1, #3, and #4 can be represented as Group B. Note that the parameters set #1 and #3 can be represented both in Group A and B simultaneously.

Figure 46 shows the difference of means for internal flatness between each set of parameters. Parameters set #1 & #2, and #3 & #4 have the closest correlation between them, whereas parameters set #2 & #3, and #2 & #4 are significantly different.

Figure 47 shows the interval plot of internal flatness for each set of parameters and the mean comparison between them. The graph shows that there are overlaps between the interval of parameters set #1 & #2 and #3 & #4, which explains the correlation of parameters set #3 from the *Tukey comparisons* chart.

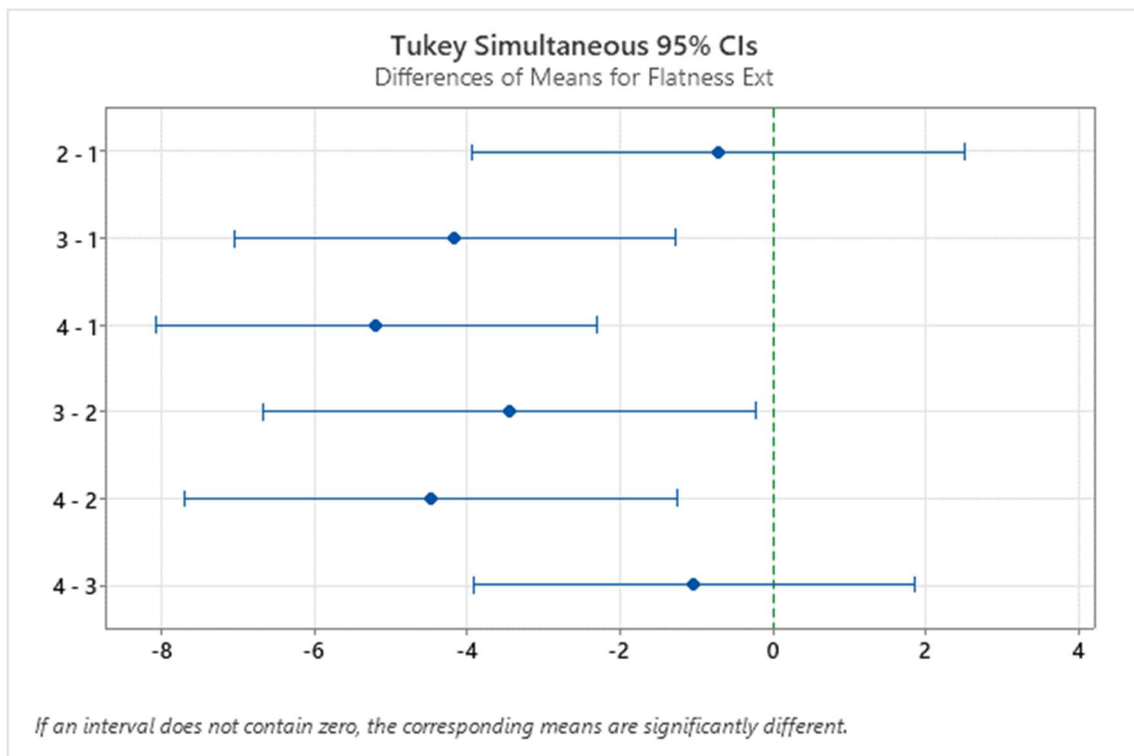


Figure 46. Differences of means of external flatness.

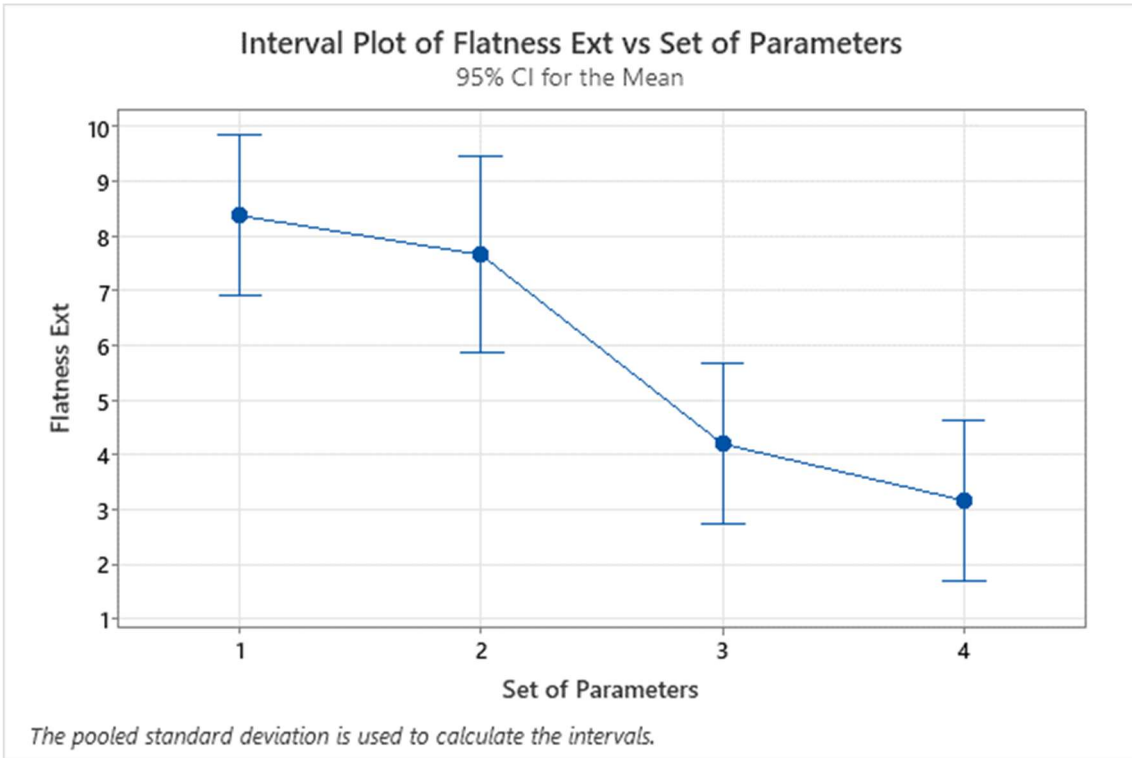


Figure 47. Interval plot of external flatness.

Figure 48 show the boxplot for each dataset, The parameters set #4 has the lowest average value of internal flatness compared to the other data. The data of parameters set #2 has very high deviation.

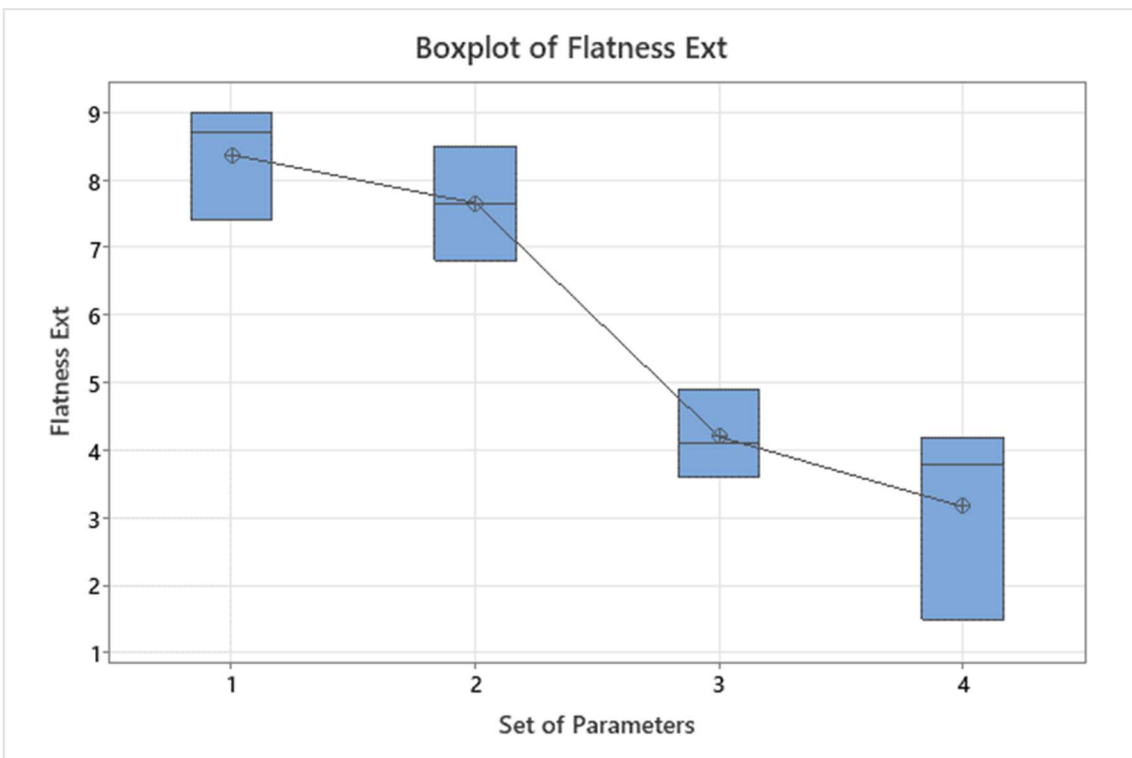


Figure 48. Boxplot of external flatness.

8.3. Process Capability

In the previous section, the parameters set #4 have been determined to have the lowest average value of the flatness of the workpiece. With that knowledge in mind, further tests were carried out to check other critical features that have been requested by the customer such as the surface finish, parallelism, thickness, and step dimensions using the set of parameters #4.

Table 7. Measurement results of the chosen set of parameters

	Flatness Int (μm)	Flatness Ext (μm)	Average Flatness (μm)	Surface Finish (μm)	Parallelism (μm)	Thickness (mm)	Step (mm)
1	1.4	2.9	2.2	0.19	18	3.951	1.931
2	4.0	6.3	5.1	0.22	17	3.950	1.831
3	1.6	2.0	1.8	0.19	11	3.951	1.894
4	2.6	1.9	2.3	0.21	10	3.939	1.857
5	4.4	6.0	5.2	0.22	12	3.946	1.837
6	2.3	2.9	2.6	0.24	10	3.947	1.900
7	2.1	4.2	3.1	0.19	17	3.943	1.856
8	2.1	5.3	3.7	0.20	12	3.954	1.944
9	0.7	1.4	1.1	0.22	10	3.942	1.921
10	3.2	1.5	2.4	0.21	10	3.942	1.922
11	4.0	5.3	4.6	0.24	10	3.942	1.841
12	2.9	4.3	3.6	0.24	10	3.947	1.864
13	3.4	5.1	4.3	0.23	9	3.951	1.843
14	1.5	3.7	2.6	0.27	16	3.955	1.890
15	3.6	4.8	4.2	0.27	10	3.942	1.957
16	2.7	3.8	3.2	0.16	9	3.950	1.839
17	3.4	4.0	3.7	0.23	16	3.942	1.883
18	3.3	3.6	3.4	0.24	9	3.942	1.891
19	3.6	5.0	4.3	0.20	15	3.950	1.846
20	4.5	4.2	4.3	0.19	10	3.946	1.917

There are 20 samples of the workpiece that have been collected in order to increase the test accuracy and to validate the process capability for each critical feature. For the process capability of the flatness, the average values are taken to simplify the analysis.

8.3.1. Process Capability for Flatness

In the process capability analysis for the flatness, the upper specification limit of 5 μm and no lower specification limit have been set, because the flatness is an absolute value, and it is better to have the value as close to zero as possible. From the analysis, the value of the *Overall Capability* (Ppk) of the process is 0.48, whereas the value of the *Potential (Within) Capability* (Cpk) of the process is 0.49 were found. It can be said that the process is not capable of producing the desired specification since the Cpk value is lower than 1.

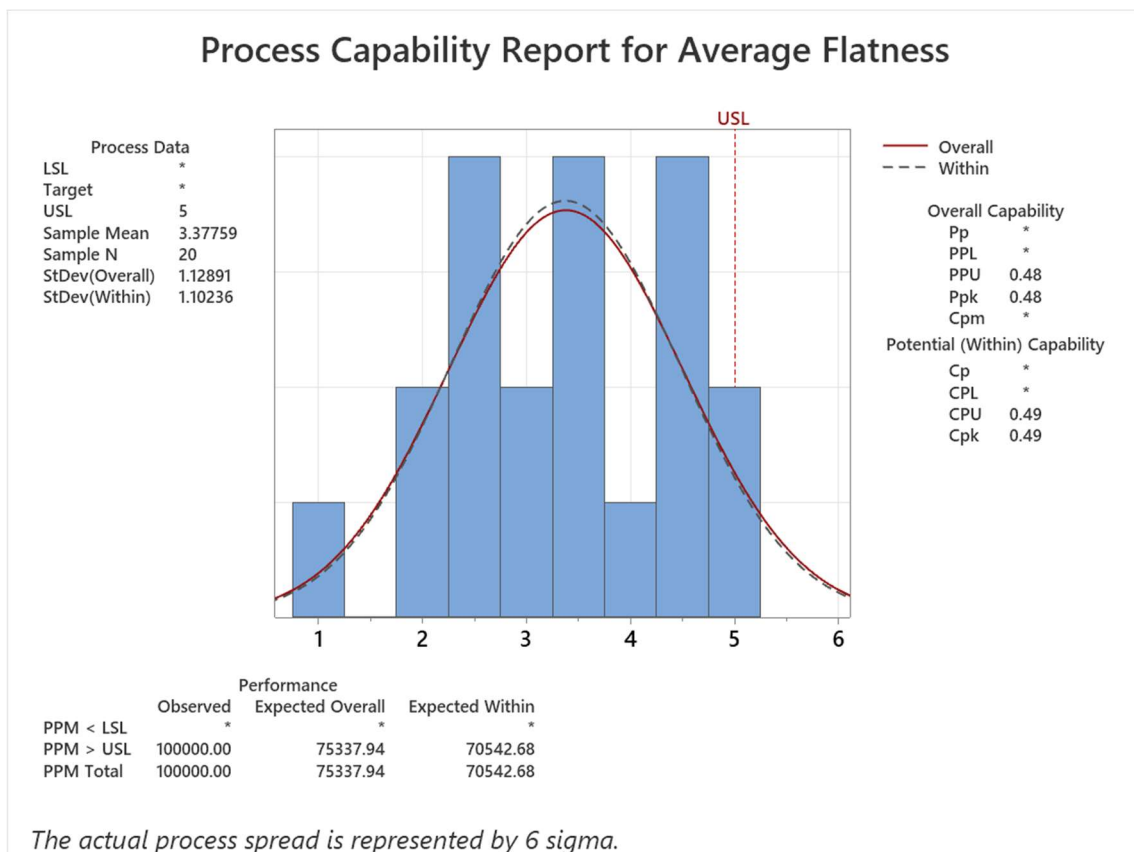


Figure 49. Process capability of average flatness.

8.3.2. Process Capability for Surface Finish

In the process capability analysis for the surface finish, the upper specification limit of 0.3 μm and 0.15 μm for the lower specification limit have been set. From the analysis, the value of the *Overall Capability* (Ppk) of the process is 0.81, whereas the value of the *Potential*

(Within) Capability (Cpk) of the process is 1.00 were found. The process is barely capable of producing within the specification.

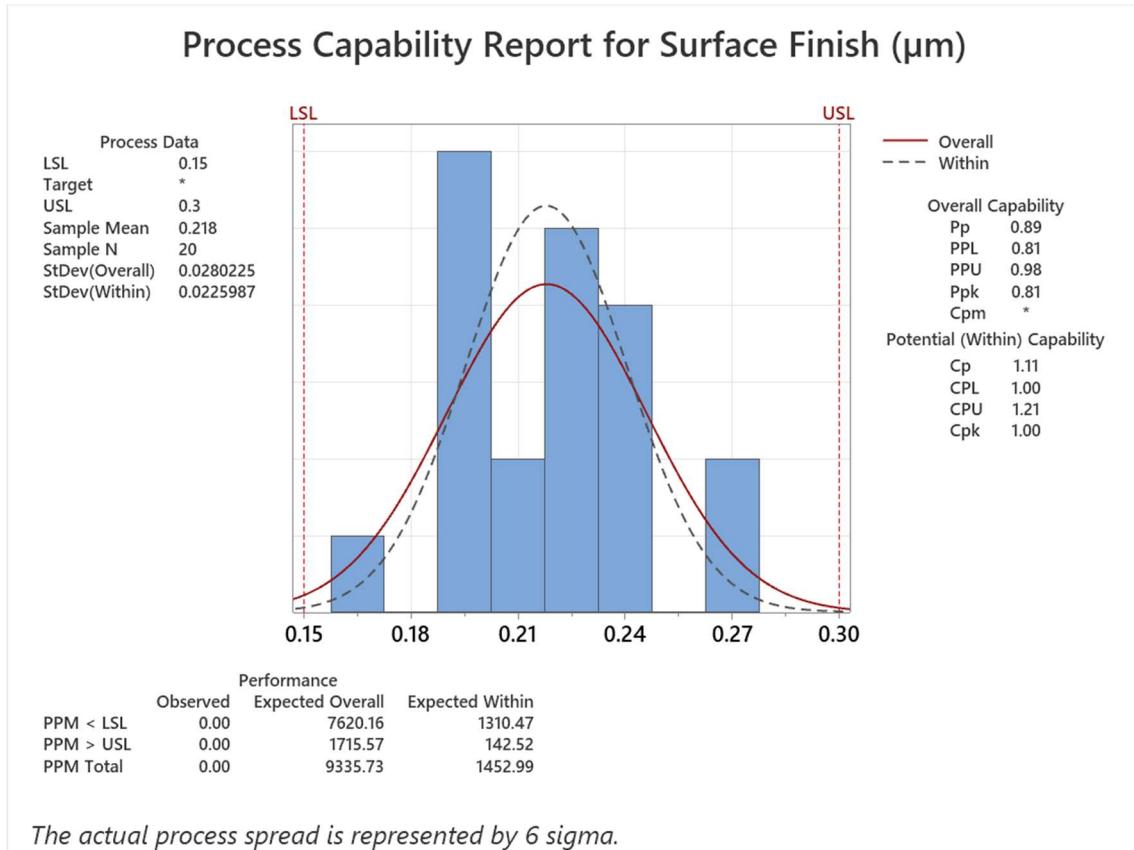


Figure 50. Process capability of surface finish.

8.3.3. Process Capability for Parallelism

In the process capability analysis for the parallelism, the upper specification limit of 0.076 mm or 76 μm and no lower specification limit have been set, because the parallelism is an absolute value, and it is better to have the value as close to zero as possible. From the analysis, the value of the *Overall Capability* (Ppk) of the process is 6.8, whereas the value of the *Potential (Within) Capability* (Cpk) of the process is 6.46 were found. This process is very capable of consistently being produced within the desired specification.

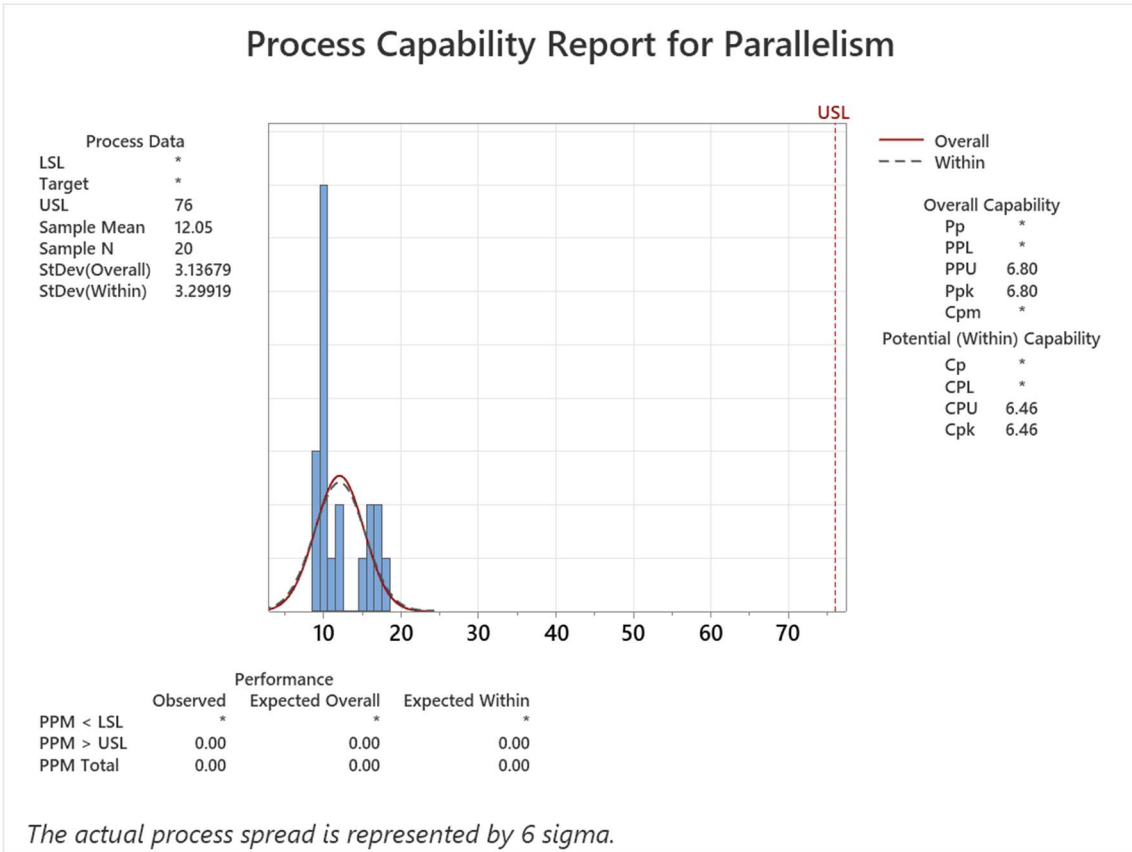


Figure 51. Process capability of parallelism.

8.3.4. Process Capability for Thickness

In the process capability analysis for the thickness, the upper specification limit of 3.96 mm and 3.92 mm for the lower specification limit have been set. From the analysis, the value of the *Overall Capability* (Ppk) of the process is 0.95, whereas the value of the *Potential (Within) Capability* (Cpk) of the process is 0.88 were found. In the current stage, the process is not capable of producing within the desired specification. However, there is a quite large buffer to the lower specification limit, which is represented by the CPL value of 1.74. It could be possible to shift the process towards the lower limit to have a more capable process.

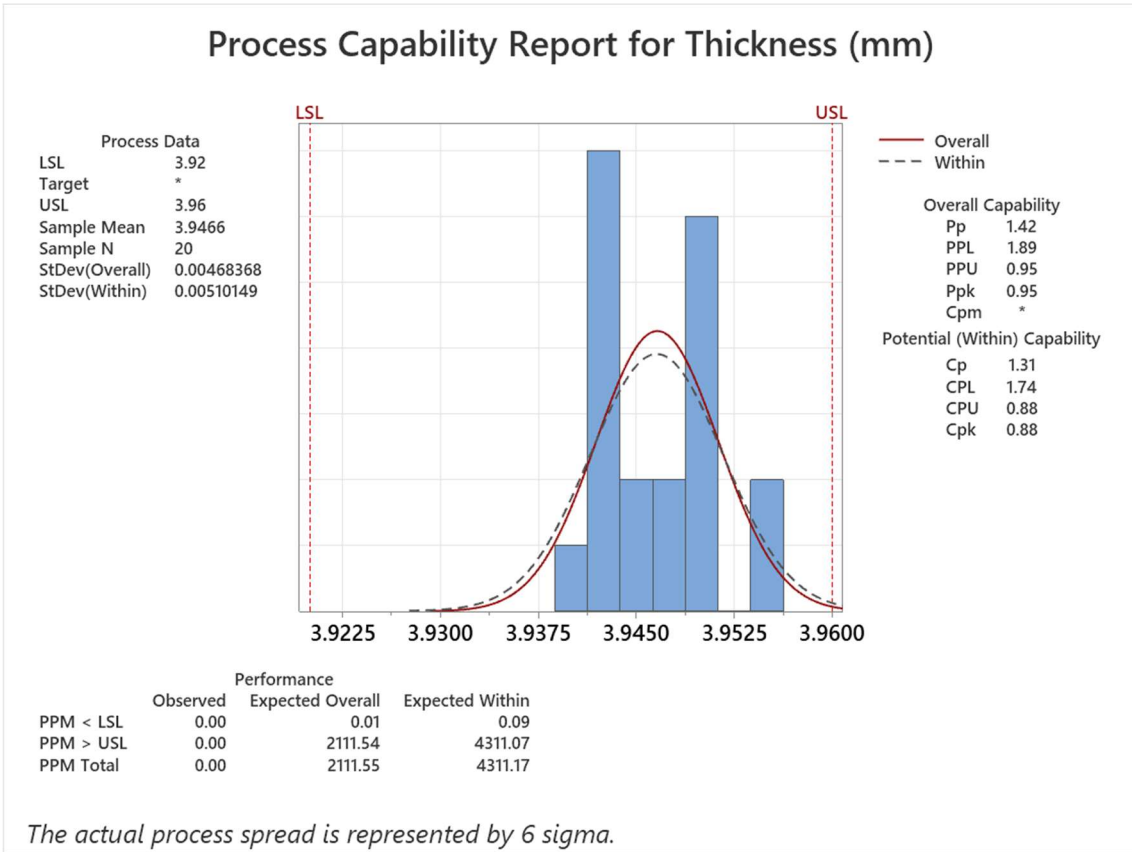


Figure 52. Process capability of thickness dimension.

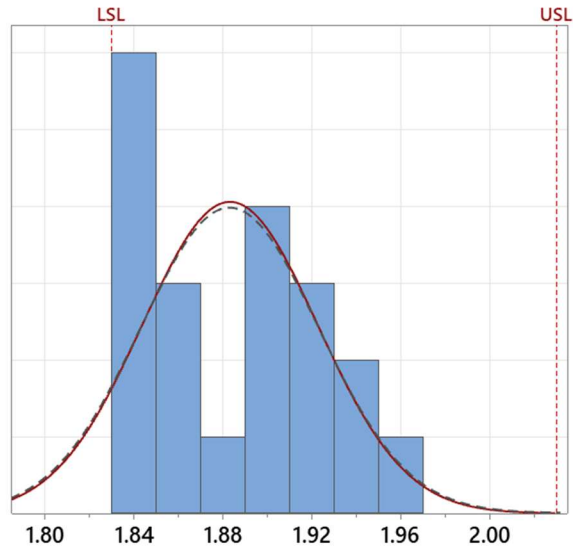
8.3.5. Process Capability for Step

In the process capability analysis for the step, the upper specification limit of 2.03 mm and 1.83 mm for the lower specification limit have been set. From the analysis, the value of the *Overall Capability* (Ppk) of the process is 0.45, whereas the value of the *Potential (Within) Capability* (Cpk) of the process is 0.44 were found. In the current stage, the process is not capable of producing within the desired specification. However, there are some buffers to the upper specification limit, which is represented by the CPU value of 1.22. It could be possible to shift the process towards the upper limit to have a more capable process.

Process Capability Report for Step (mm)

Process Data

LSL 1.83
 Target *
 USL 2.03
 Sample Mean 1.8832
 Sample N 20
 StDev(Overall) 0.0393361
 StDev(Within) 0.0400653



— Overall
 - - - Within

Overall Capability
 Pp 0.85
 PPL 0.45
 PPU 1.24
 Ppk 0.45
 Cpm *

Potential (Within) Capability
 Cp 0.83
 CPL 0.44
 CPU 1.22
 Cpk 0.44

Performance

	Observed	Expected Overall	Expected Within
PPM < LSL	0.00	88115.97	92116.96
PPM > USL	0.00	95.00	124.15
PPM Total	0.00	88210.98	92241.11

The actual process spread is represented by 6 sigma.

Figure 53. Process capability of step dimension.

9. Discussion and Conclusion

In the beginning phase of machine design, the overhang value (Δ_0) that affected WCR has been chosen as 5 mm by the company's engineer, which gives the test configuration WCR value of 0.876. By comparing it to the study of Dražumerič et. al. (7), the WCR value of 0.876 is rather high and can lead to stoppage of workpiece self-rotating mechanism. It will be interesting to study this mechanism further with the company's test configuration to see whether 5 mm overhang is sufficient to induce the self-rotating mechanism, and whether the self-rotating mechanism can lead to better surface flatness of the workpiece.

The choice of parameters set that were used for the test is based on the experience of the machine operator to save time and satisfied the deadline proposed by the client. However, the testing methodology and the choice of parameter values could be improved from scientific point of view to further optimize the grinding process. Obviously, with a more sophisticated test methodology, there must be more time dedicated to accomplishing the test, which might not be available in the company's schedule.

In the case of process capability of the grinding process, out of five important requirements, only one requirement that can be confidently achieved within the specification (Parallelism), two requirements that can be barely achieved within the specification (Surface Finish and Thickness Dimension), and the other two requirements that cannot be confidently achieved within the specification (Average Flatness and Step Dimension). It should be noted that for the average flatness specification, the USL value of 5 μm is defined by the company, and the actual specification required by the client (0.8 μm) can only be achieved after lapping process, which is not covered in this test. In the case of thickness and step dimensions, the distribution diagrams show that both standard deviations are within the LSL and USL values, thus, it is the matter of fine-tuning the machine in order to improve its process capability to be more consistent.

Unfortunately, during the writing of this thesis, the client has not decided whether they will use the Viotto Grinding Machine for their grinding application or not.

From the testing activity that has been carried out, it is possible to draw some conclusions:

- The parameters used to deliver the best result are modified grinding wheel openings (0.21 longitudinal, 0.19 transversal), top grinding wheel speed of 120 RPM, bottom grinding wheel speed of 1200 RPM, and rotary table speed of 1.66 RPM.
- The production rate achieved by the machine is 60 pieces per minute.
- The finished workpiece parallelism is excellent with respect to the customer requirements.
- The finished workpiece surface finish is adequate to the customer requirement.
- The finished workpiece thickness is close to the customer requirement with small refinement is needed.
- Further testing and adjustment are required to achieve the desired value of workpiece flatness and step dimension.

References

1. **Marinescu, Ioan D., et al.** *Handbook of Machining with Grinding Wheels*. Boca Raton : Taylor & Francis Group, 2007.
2. **Kalpakjian, Serope and Schmid, Steven R.** *Manufacturing Engineering and Technology*. Harlow : Pearson Education Limited, 2023.
3. **Universal Grinding Corporation.** *Universal Grinding: Mastering the Craft of Grinding for Precision and Efficiency*. *Universal Grinding*. [Online] Universal Grinding Corporation. [Cited: 15 July 2023.] <https://universalgrinding.com/universal-grinding-mastering-the-craft-of-grinding-for-precision-and-efficiency/>.
4. **Groover, Mikell P.** *Fundamentals of Modern Manufacturing*. Hoboken : John Wiley & Sons, Inc., 2010.
5. **Wember, Dirk .** XING dressing: a dressing technique for tapered [or V-shaped] diamond grinding wheels. *A.HAAS*. [Online] Adelbert Haas GmbH, 26 October 2017.
6. **Diamant-Gesellschaft Tesch GmbH.** Grinding Tools Products. *Diamant-Gesellschaft Tesch GmbH*. [Online] [Cited: 12 July 2023.] <https://www.diamanttesch.de/en/schleifwerkzeuge>.
7. *Mechanics of Self-rotating Double-disc Grinding Process*. **Drazumeric, Radovan, et al.** San Antonio : Elsevier, 2022.
8. *Analysis and simulation of double disc grinding*. **Shanbhag, Nilesh, et al.** TECHNICAL PAPERS-SOCIETY OF MANUFACTURING ENGINEERS-ALL SERIES, 1998.
9. **Minitab.** Minitab Getting Started. *Minitab*. [Online] [Cited: 23 August 2023.] https://www.google.com/url?sa=t&rct=j&q=&esrc=s&source=web&cd=&cad=rja&uact=8&ved=2ahUKEwiWs-6RjtODAxWR7DgGHZ_QDJUQFnoECAsQAQ&url=https%3A%2F%2Fwww.minitab.com%2Fcontent%2Fdam%2Fwww%2Fen%2Fuploadedfiles%2Fdocuments%2Fgetting-started%2FMinitabGettingStarte.